2-DIMENSIONAL FLOOD CONTROL SIMULATIONS FOR WAMI AND DÜDEN RIVERS

A THESIS SUBMITTED TO
THE GRADUATE SCHOOL OF NATURAL AND APPLIED SCIENCES
OF
MIDDLE EAST TECHNICAL UNIVERSITY

BY

UĞUR CAN KARAKUŞ

IN PARTIAL FULFILLMENT OF THE REQUIREMENTS
FOR
THE DEGREE OF MASTER OF SCIENCE
IN
CIVIL ENGINEERING

SEPTEMBER 2019

Approval of the thesis:

2-DIMENSIONAL FLOOD CONTROL SIMULATIONS FOR WAMI AND DÜDEN RIVERS

submitted by **UĞUR CAN KARAKUŞ** in partial fulfillment of the requirements for the degree of **Master of Science in Civil Engineering Department, Middle East Technical University** by,

Prof. Dr. Halil Kalıpçılar
Dean, Graduate School of **Natural and Applied Sciences** _____

Prof. Dr. Ahmet Türer
Head of Department, **Civil Engineering** _____

Prof. Dr. Zafer Bozkuş
Supervisor, **Civil Engineering, METU** _____

Examining Committee Members:

Prof. Dr. İsmail Aydın
Civil Engineering, METU _____

Prof. Dr. Zafer Bozkuş
Civil Engineering, METU _____

Prof. Dr. Zuhal Akyürek
Civil Engineering, METU _____

Assoc. Prof. Dr. Yakup Darama
Civil Engineering, Atılım University _____

Assist. Prof. Dr. Meriç Yılmaz
Civil Engineering, Atılım University _____

Date: 12.09.2019

I hereby declare that all information in this document has been obtained and presented in accordance with academic rules and ethical conduct. I also declare that, as required by these rules and conduct, I have fully cited and referenced all material and results that are not original to this work.

Name, Surname: Uğur Can Karakuş

Signature:

ABSTRACT

2-DIMENSIONAL FLOOD CONTROL SIMULATIONS FOR WAMI AND DÜDEN RIVERS

Karakuş, Uğur Can
Master of Science, Civil Engineering
Supervisor: Prof. Dr. Zafer Bozkuş

September 2019, 83 pages

In this study, flood scenarios of bridge sections of Wami and Düden Rivers are examined with 2D flood modelling. HEC-RAS 2D software is used for the flood simulations. The bridge locations are investigated to protect against hazardous floods expected in the regions. For Wami Bridge, three scenarios are examined; existing case (where only the operated bridge is modelled), design case (where the newly designed bridge is added) and modified design case (where channel modification is introduced with both bridges). For Düden Bridge, existing case (where the historical bridge with insufficient openings) and modified case (where an adjoint bypass channel sharing the flood discharge) are simulated. In the analyzes, instead of 1D modelling, 2D modelling is preferred because of the flat topographic characteristics of the regions, absence of defined riverbed and parallel channels with different slope profiles. For Wami Bridge, using trapezoidal channelization with 15-m width and 2-m depth, the water height at the designed bridge is lowered to 1.45 m and the discharge capacity is increased to 100.74 m^3/s while the discharge capacity of the existing bridge is increased from 20.40 m^3/s to 100.63 m^3/s. For Düden Bridge, using a rectangular by-pass channel, the water height at the historical bridge is lowered to 3.40 m, at which the historical bridge will enable the passage of $Q_{Düden}$ = 110.69 m^3/s and the bypass channel will carry the rest

of the flood, that is, Q_{bypass} = 141.19 m^3/s. As a result, the flood control alternatives with hydraulically appropriate solutions were identified for both cases.

Keywords: Flood, Flood Modelling, HEC-RAS, HEC-RAS 2D, Düden, Antalya, Wami, Tanzania

ÖZ

WAMİ VE DÜDEN NEHİRLERİ İÇİN 2-BOYUTLU TAŞKIN MODELLENMESİ

Karakuş, Uğur Can
Yüksek Lisans, İnşaat Mühendisliği
Tez Danışmanı: Prof. Dr. Zafer Bozkuş

Eylül 2019, 83 sayfa

Bu tez çalışmasında, Wami ve Düden Nehirlerinin taşkın senaryoları, iki farklı köprü bölgesi için iki boyutlu modellenerek incelenmiştir. Taşkın simülasyonları için HEC-RAS 2D yazılımı kullanılmıştır. Bölgelerde beklenen tehlikeli sel baskınlarına karşı koruma sağlamak için iki köprü yeri araştırılmıştır. Wami Köprüsü için ise üç farklı senaryo incelenmiştir; mevcut durum (sadece mevcut işletmedeki köprü), tasarım durumu (mevcut ve tasarlanan köprü) ve değiştirilmiş tasarım durumu (iki köprü ile birlikte kanal modifikasyonu). Düden Köprüsü için mevcut durum (yetersiz kapasiteli tarihi köprü) ve değiştirilmiş durum (taşkın debisini paylaşan paralel bypass kanalı) modellenmiştir. Analizlerde, 1B modelleme yerine, bölgelerin düz topografik özellikleri, belirgin nehir yatağının bulunmaması ve farklı akış rejimlerindeki parallel kanalların bulunması nedeniyle 2B modelleme tercih edilmiştir. Wami Köprüsü için, 15-m genişliğinde ve 2-m derinliğinde kanal modifikasyonu yapılarak, dizayn edilen köprünün, deşarj kapasitesi 100.74 m^3/s'ye, mevcut köprünün deşarj kapasitesi ise 20.40 m^3/s'den 100.63 m^3/s'ye yükseltilmiştir. Düden Köprüsü için, dikdörtgen bir by-pass kanalı mevcut nehir yatağına pararlel olarak dizayn edilerek, tarihi köprüdeki taşkın su yüksekliği 3.40 m'ye düşürülmüştür. Taşkının Qbypass=141.19 m^3/s'lik kısmı by-pass kanalı ile taşınmış ve köprüdeki taşkın geçişi QDüden=110.69 m^3/s'ye

indirilmiştir. Simulasyonlar sonucunda, hidrolik olarak uygun taşkın kontrol çözümleri belirlenmiştir.

Anahtar Kelimeler: Taşkın, Taşkın Modelleme, HEC-RAS, HEC-RAS 2 Boyutlu Modelleme, Düden, Antalya, Wami, Tanzanya

To My Mother

ACKNOWLEDGEMENTS

This thesis was completed under the supervision of Prof. Dr. Zafer Bozkuş. First and foremost, I would like to offer him my deepest gratitudes, not only for his support and guidance during the course of this work, but also for presenting me with the opportunity to work on this study which brought my profession, civil engineering, together with my enthusiasm, history and water sciences.

I would like to thank the jury members of my thesis, Prof. Dr. İsmail Aydın, Prof. Dr. Zuhal Akyürek, Assoc. Prof. Dr. Yakup Darama, and Assist. Prof. Dr. Meriç Yılmaz for their contributions and interest in my work.

I also would like to extend my thanks to all my workmates at TEMELSU for all the assistance and providing the project data. Their evaluations and contributions for the thesis are gratefully acknowledged.

I wish to express my gratefulness to my parents, Aytop Sönmez Karakuş and Halil İbrahim Karakuş, along with my brother, Onur Cem and his spouse, Sinem, for their endless encouragements and moral support.

I gratefully acknowledge Burak Uçak, Onur Deniz Uysal, Umut Kara, Emine Deniz Özdamar, Selin Özdemir and Emre Dede for their assistance and patience throughout my studies, Barış Ünal, Zeynep Ünal and Bahadır Bilgin for cheering me up on Discord when I was on the rack at Tanzania and Sedenay Akbaş for her unearthly optimism and unlimited support. Similarly, I would like to thank to all my colleague for their motivation and tolerance.

TABLE OF CONTENTS

LIST OF TABLES

TABLES

LIST OF FIGURES

FIGURES

CHAPTER 1

INTRODUCTION

1.1. Background

A flood is an uncommonly high stage of a stream and it is considered to be some of the most significant natural hazards in the world. For a stream in its natural state, the occurrence of a flood usually fills the stream up to its banks and often spills over to the neighboring flood plains. Most commonly, it occurs after a heavy rainfall when natural watercourses do not have the capacity to carry excess water.

A floodplain is an area of land adjacent to a stream or river which stretches from the banks of its channel to the base of the enclosing valley walls, and which experiences flooding during periods of high discharge.

Flooding can be categorized into three groups; (1) Fluvial floods, (2) pluvial floods and (3) coastal floods. The most common one is fluvial floods, caused when the water surface of a river is rising above its riverbanks, flooding nearby areas. Fluvial floods are controlled by hydrological processes such as precipitation or evaporation, occurring over large temporal and spatial scales, and typically occur after periods of sustained rainfall. On the other hand, the pluvial floods occur when the intensity of the rain exceeds the infiltration capacity of the ground, resulting in an overland flow. Coastal floods are caused by increases in seawater levels due to set up from winds, waves, climate change affecting low elevation land next to seas.

1.2. Aim of the Thesis

The general objective of this thesis is to study flood simulations for the historical bridge sections to define the hydraulic capacity and adequacy changes with the aid of 2D modeling, using actual hydrological and geometrical data and to identify proper

flood protection strategies. In this aspect, Düden River in Turkey and Wami River in Tanzania are examined as case studies of the thesis.

Düden bridge is a historical Seljuk era bridge of the Düden River in Antalya, Turkey. The origin of the bridge is not completely known. From architectural inspections, it is estimated to be built in the early 13th century. The only written information about the bridge is, Kadı Süleyman's foundation certificate-charter, which is from the 16th century. It is written in the document that some collected revenue had been spent on the repair of the bridge. The bridge has two names, Düden or Cırnık, both used in this study.

Düden River is one of the many major rivers of Antalya. The river travels underground from the source at Kırkgöz Lake and surfaces near Varsak City. It then submerges again and resurfaces where the waters of the Düden Falls drop 40 meters from a rocky cliff directly into the Mediterranean Sea. The historical Düden Bridge is located at Muratpaşa, Antalya, parallel to a bridge of Mersin-Antalya Motorway.

Global warming, deforestation and urbanization are the three of the main reasons that increase the peak flood discharges thereby causing inadequacy in the bridge capacities. Without necessary countermeasures, historical bridges may be damaged by scouring caused by high velocities or overtopping with higher water levels even if they were thoroughly designed. With the aid of 2D hydrodynamic modeling, flood regulation alternatives can be investigated for the bridge sections. Considering the flood impact on the Düden Bridge, the expected damage can be decreased to reasonable levels this way.

On the other hand, Wami bridge is a newly designed railway bridge for Morogoro-Dodoma-Makutupora railway project in Tanzania. The bridge is for a single lined railway located parallelly upstream of an existing railway. There is not a well-defined riverbed at the bridge location and the region is mostly flat, hence, the inundation area is very wide for the designed bridge region. In addition to this, the cross-section of the existing bridge is mostly filled with sedimentation, blocking any passing water from

a designed bridge located 20 m upstream, increasing the backwater in the case of flood.

Wami River lies within Tanzania in the Pwani Region and Morogoro Region in eastern Tanzania. Its source is located in the Kaguru Mountains and it flows East entering the Indian Ocean west of Zanzibar. The bridge is located approximately 20 km west of Morogoro City.

In this case, 2D hydrodynamic modeling utilized to analyze the inundation area boundaries and channelization alternatives for the area to improve the discharge capacity of the designed and existing railway bridges.

1.3. Method

In this study, the numerical floodplain models of the rivers has been constructed by river analysis software HEC-RAS, which enables users to perform water surface elevation calculations. HEC-RAS can perform one-dimensional and two-dimensional flow calculations. 1D models can represent the flow successfully if the flow path is well defined and spread is limited. However, for rivers with wide and complex floodplains, and significant cross-section variation, modeling can be done more realistically in 2D.

CHAPTER 2

LITERATURE REVIEW

The flood risk is the probability of occurrence of a flood, vulnerability to flood and exposure to flood. If there are enough measurement periods for flood occurrence, it is easy to generate the probability of occurrence of a flood. Even if there is enough record for peak flows, the probability can be generated by a simple peak discharge frequency analysis. The vulnerability relates to potential consequences in case of an event and in flood cases, the potential consequences can be missing people, agricultural damage, building damage, loss of agricultural land, river fisheries, dams, etc. (Vlek, 1996; UN-ISDR, 2007; Smith, 2001).

The models are different from each other according to how the channels are routed, the discretization/incorporation of the topography data and reproduction of the surface roughness. The surface roughness has great importance when discussing urban areas with a heterogeneous built-up surface (Messner and Meyer, 2005).

The storage cell models are generally considered as the least complex approaches. The models split the valley or the floodplain into single cells (Cunge, Holly and Verwey, 1980) or the more complex representations such as polygonal-shaped cells or Triangular Irregular Networks (TINs). The size of the model and the amount of detail depending on the resolution of the Digital Topography Model (DTM) and the software resources that are available (Messner and Meyer 2005). Examples for developed models are FloodWatch, FLOODSIM, Lisflood (Bates and De Roo, 2000).

On the other hand, hydrological data used in the simulations is another important part of a flood model. In 2012, Bostan, Heuvelink and Akyurek compared five different statistical methods (multiple linear regression (MLR), ordinary kriging (OK), regression kriging (RK), universal kriging (UK), and geographically weighted

regression (GWR)) to predict spatially the average annual precipitation of Turkey using point observations of annual precipitation at meteorological stations and spatially exhaustive covariate data. UK has found to be the most reliable method for spatial interpolation of precipitation distribution (Bostan, Heuvelink, & Akyurek, 2012).

The applications of HEC-RAS and HEC-RAS 2D are common in flood modeling in all over the world. Mišík, Bajčan, Sklenář, and Kučera (2013) carried out a project in city Prague. The city was affected by flood events a lot of time, the last one was in June 2013. An important part of flood protection measures in city Prague is mobile flood barriers along banks of river Vltava. The mobile flood barriers would fail eventually, and they could cause flooding. It was decided that contingency planning and crisis management for such situations would be prepared based on numerical simulation of flood protection failure scenarios. Critical places of flood protection hypothetical failures were assessed, and unfavorable discharge and water level scenarios were prepared. Flooding of most vulnerable urban areas was simulated by 2-D hydrodynamic unsteady flow modeling. Selected localities were defined with scenarios of flooding through sewer system manholes. Results of simulations were presented in form of maps showing flooding extent, inundation depth, water surface elevations, flow velocity magnitudes and directions, as well as by text description of the flooding situation, all in selected time steps. Video animations showing flooding evolution in space and time were created. All results were elaborated in the form of an interactive graphical application, which helps planners and crisis managers at the city level.

In 2015, Yeğin demonstrated the application of a methodology to prepare flood damage maps and flood risk maps for economic, social and environmental dimensions of risk. In the study, flood risk maps showed the flood vulnerable areas to be used to identify and design necessary precautions and prioritize areas that need attention. It is understood that they can be useful for preparing emergency planning for flood-prone

areas. The examples where residential areas are built in the riverbed in Turkey identified in the study (Yeğin, 2015).

Neal, Schumann and Bates (2012) used subgrid solver of LISFLOOD-FP for the flood inundation problem of Niger Inland Delta in Mali, concluding that including subgrid channels on the floodplain changed the inundation patterns over the delta. Özdemir, Bates and Almeida (2018) studied 4 different scenarios for the urban area of Alcester (Warwickshire, UK) stating that preventing and mitigating the flood were heavily depended on the sewage system. 1D and 2D models have been studied for the 2009 flood event in Ayamama River (İstanbul, Turkey). Both HEC-RAS and LOSFLOOD-FP-Roe model results were compared with the actual flood content (Özdemir, Neal, Bates and Döker 2013). A hypothetical small area in Terme Town, Samsun has been studied to present the effect of the spatial resolution of DEM in shallow water solutions. The results showed that increasing the resolution enabled and improved the representation of the topography (Nimaev, 2015). And most recently, Kıyıcı (2019) studied the sensitivity of a 2D hydraulic model by using LISFLOOD-FP for Terme City, (Samsun, Turkey) which exposed to a storm in 2012. The results showed that model calibration can be done by adjusting the roughness coefficient to have better results and Subgrid Channel Solver gives better results compared to Acceleration Solver because the channels can be defined with finer resolutions which eliminated the resampling problems.

CHAPTER 3

METHODOLOGY

3.1. Flood Modelling

The effects of fluvial and pluvial flood cases have been computed by hydraulic models for many years. With different governing equations and numerical solutions, there are various types of models that are being used. Usually, 1D river models are used to model fluvial flooding events. 1D models are made up of a series of cross sections describing the topography of the river and floodplain, and water levels are calculated using the one-dimensional form of the governing equations. 1D models only require topographical data to be collected at the cross sections that make up the model, which was a major advantage when access to topographic data was limited and only cross-section information is available (Betsholtz and Nordlöf, 2017).

2D hydraulic models consist of a two-dimensional computational grid, representing the topography of the region by cells. In contrast to 1D, 2D models cannot work with cross sections. It is mandatory to have continuous topographical data, covering the whole area that is to be modeled. Although the flows in a natural environment are always 3D one can take the advantage of simplified 1D or 2D mathematical models in order to achieve practical and quick solutions for engineering applications (İşcen, Öktem, Yılmaz and Aydın, 2017).

3.2. Unsteady Flood Routing

Navier-Stokes equations are the main computation formula for all unsteady flow simulations for incompressible fluids. While these governing equations are applicable in almost all situations, computational constraints typically dictate the degree of simulation detail achieved. Three-dimensional hydrodynamic modeling at the reach scale is typically unjustifiable when parameters of velocity direction and magnitude,

inundation extent, and water depth can be predicted using one-dimensional (1D) or two-dimensional (2D) computational fluid dynamics (CFD) (Bates and De Roo, 2000; Piotrowski, 2010).

3.3. One-Dimensional Unsteady Flood Models

The simplest way of representing floodplain is to assume that the flow is one-dimensional along the center of the river. This approach is very useful if either a more detailed study is unnecessary, or the flow is inside of a confined channel. The most widely used approach for modeling fluvial hydraulics has been 1D finite difference solutions of the full Saint-Venant Equations (Bates and De Roo, 2000).

Conservation of mass

$$\frac{dQ}{dx} + \frac{dA}{dt} = 0 \tag{3.1}$$

Conservation of momentum

$$\frac{1}{A}\frac{dQ}{dt} + \frac{1}{A}\frac{d(Q^2/A)}{dx} + g\frac{dh}{dx} - g(S_0 - S_f) = 0 \tag{3.2}$$

Where Q is flow discharge, t is time, h is water depth, g is the gravitational acceleration, S_f is the slope of friction and S_0 channel bed slope.

One-dimensional solutions of the full Saint-Venant Equations are derived based on several assumptions: the flow is one-dimensional, the water level across the section is horizontal, the streamline curvature is small and vertical accelerations are negligible, the effects of boundary friction and turbulence can be accounted for using resistance laws analogous to those for steady flow conditions, and the average channel bed slope is small so the cosine of the angle can be replaced by unity (Cunge, Holly and Verwey, 1980).

3.4. Two-Dimensional Unsteady Flood Models

2D hydrodynamic models are the most widely used models in flood extent mapping and flood risk estimation studies. A complex interaction of channel and floodplain flow fields make two-dimensional simulations more effective than one-dimensional simulations in many modeling works. The most widely used two-dimensional modeling softwares utilize the Saint-Venant shallow water equations, obtained by depth-averaging Navier-Stokes equations (Néelz, Pender and Wright 2010).

Conservation of mass

$$\frac{dh}{dt} + \frac{d(hu)}{dx} + \frac{d(hv)}{dy} = 0 \tag{3.2}$$

Conservation of momentum

$$\frac{d(hu)}{dt} + \frac{d}{dx}\left(hu^2 + \frac{1}{2}gh^2\right) + \frac{d(huv)}{dy} = 0 \tag{3.3}$$

$$\frac{d(hv)}{dt} + \frac{d(huv)}{dx} + \frac{d}{dy}\left(hv^2 + \frac{1}{2}gh^2\right) = 0 \tag{3.4}$$

Where x and y are the two spatial dimensions, and the 2D vector is the horizontal velocity averaged across the vertical column. The solution of these equations comprises estimates of u, v, and h over space and time.

As with the one-dimensional Saint-Venant equations, the two-dimensional shallow water equations (SWE) have no analytical solutions. The SWE system, based on the integration of the Navier-Stokes equations in the vertical direction, consists of the continuity and two horizontal momentum equations (İşcen et al., 2017).

Depending on numerical mesh/grid generation strategies, the models can be classified into finite element, finite difference, and finite volume methods.

According to decomposing in time, the models can be divided into implicit (solver cannot proceed to the next time step until the whole domain is solved) and explicit (solving of the current unit independent of solving the rest of the domain for any given time step) models.

In terms of spatial representation, the models can use a structured mesh (rectangular grids), unstructured mesh (triangular grids), and most recently, flexible mesh (HEC-RAS) which is used in this study.

In the 2D hydrodynamic models, the assumption that the vertical velocities are negligible might be inaccurate, at least when modeling channel flow. The diffusive wave simplification has been used in many of the simulations performed in this study. Using this simplification all acceleration and turbulence terms are neglected, which might not be accurate when modeling flow in channels or on complex floodplains. In addition to the uncertainties regarding the applicability of the governing equations, there is some additional uncertainty related to the numerical solution of the equations. The numerical solvers all have some tolerance for errors, and the solution does not always converge, which might cause mass balance errors. (Betsholtz & Nordlöf, 2017)

HEC-RAS 2D uses both finite difference and finite volume scheme to numerically integrate shallow water equations. The computation time intervals had been selected in such a way that the Courant number is less than 1.0 for an accurate and stable solution. Selecting an adequate time step is a function of the cell size and the velocity of the flow moving through those cells.

3.5. Courant Time Step Calibration

The Courant–Friedrichs–Lewy or CFL condition is a term for the stability of unstable numerical methods that model convection or wave phenomena by an article by Courant, Friedrichs, and Lewy introduced in 1928. This derivation is known for its influence on the development of computational fluid dynamics techniques.

The CFL condition expresses that the distance that any information travels during the timestep length within the mesh must be lower than the distance between mesh elements. In other words, information from a given cell or mesh element must propagate only to its immediate neighbors. The CFL condition can be derived in a simple way, considering the simple linear convection problem of a quantity u:

$$\frac{du}{dt} + a\frac{du}{dx} = 0 \tag{3.5}$$

For the simple problem of linear convection of a quantity u, the first order explicit scheme:

$$\frac{u_i^{n+1} - u_i^n}{\Delta t} + \frac{a}{\Delta x}(u_i^n - u_{i-1}^n) = 0 \tag{3.6}$$

where a is the velocity magnitude, Δt is the timestep and Δx is the length between mesh elements.

By performing a Taylor series expansion on this scheme, this scheme introduces what is called a numerical diffusion, or numerical viscosity, equal to:

$$\mu_{num} = a\frac{\Delta x}{\Delta 2}\left(1 - \frac{a\Delta t}{\Delta x}\right) \tag{3.7}$$

As expected from a diffusion coefficient, the numerical diffusion coefficient must be positive, otherwise, the solution will grow indefinitely with respect to time, making the numerical scheme unstable.

The right term inside the parenthesis of the above expression is commonly referred to as the Courant number, which is a dimensionless quantity. Therefore, the Courant number can be stated as follows:

$$C = v\frac{\Delta t}{\Delta x} \leq 1.0 \tag{3.8}$$

Where C is Courant Number, v flow velocity (m/s), Δt is computational time step (s) and Δx is average cell size (m). Courant number must be equal or smaller than 1, otherwise, the numerical viscosity would be negative. Meaning that the water should not flow between cross sections of two grids or pass from one to another within one time-step.

3.6. HEC-RAS 2D Modelling

Computer modeling techniques have been widely used in water related studies. Engineers may determine the occurred area and results of the floods by using these modeling tools. Computer modeling techniques have assisted engineers in determining where and when flooding may occur more accurately (Snead, 2000).

There are four steps in flood area determination based on computer models:

Pre-processing: Preparation of the data as model input, such as Digital Elevation Model (DEM) of the area, hydrological inputs, such as precipitation, discharge measurement and roughness of the riverbed.

Hydrologic Studies: Calculation of flood hydrographs or flood peak discharges depending on the scope and the available data for studies.

Hydraulic Modeling: A hydraulic model to determine water surface profiles at the study area.

Post processing: Floodplain mapping and visualization of the results (Onuşluel, 2005).

There are various types of computer models for computations of water surface profiles. Each program has a specific interface for mapping the results. A collective tool for the result maps is needed for easy comparison and common use. The interaction for such software in numerical models has a great advantage. Such as MIKE by DHI used in this study has a Geographic Information Systems (GIS) interaction, which eases the interpretation of the results.

Geographic Information Systems (GIS) tool offering the ideal environment for this type of work is widely used in floodplain delineation studies. GIS offers engineers a powerful capability to analyze and to express visually flood measures.

GIS is an excellent tool for the management of results and calculations. However, it cannot be used for flood modeling. GIS can be used with a flood simulation model to delineate flood areas. GIS has several advantages for flood model studies such as; it is possible to integrate data from different sources and the display, data organizing capabilities of GIS are powerful.

3.6.1. Mesh Construction and Features

The 2D geometry is built up by a computational mesh (or computational grid), illustrated in Figure 3.1. Each mesh is built up by interconnected cells that may vary in size and shape, although one cell cannot have more than 8 cell faces. Cell faces are used to compute flow between cells, except at the outer boundaries of the mesh. Cell points, located at the connection between cell faces, are used to connect the mesh to 1D structures and 2D boundary conditions. The cell center is where the water surface elevation is computed for each cell but doesn't necessarily correspond to the cell centroid.

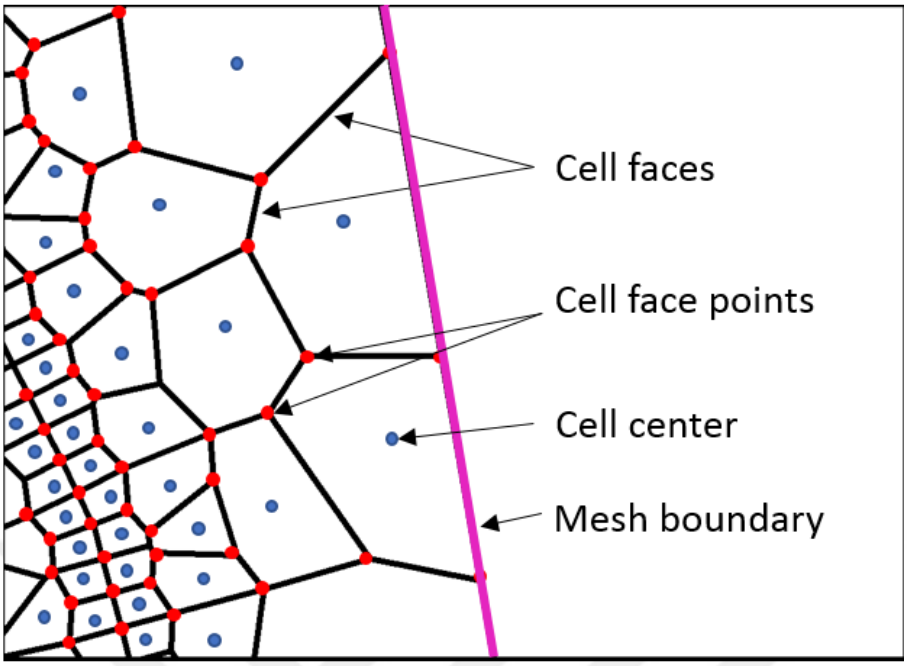

Figure 3.1. Illustration of a computational mesh/grid

3.6.2. Sub-grid Terrain Representation

Compared to many other 2D modeling software, HEC-RAS cells and cell faces can contain not only elevation value, but they can also have detailed geometric and hydraulic property tables, based on the resolution of the underlying terrain, are created during pre-processing of the computational mesh. For each cell face, relationships between elevation and profile, area, wetted perimeter, and Manning's n are computed. For each computational cell, a relationship between elevation and volume is computed.

This method of representing the terrain is referred to as a "high-resolution sub-grid model", a technique developed by Casulli (2009). The idea is to be able to increase the cell size of the computational mesh (reduce computation times) without losing too much important information regarding the underlying terrain. One disadvantage of using the sub-grid representation is that only cell faces will capture the terrain profile. Features within the terrain will only be represented by the volume elevation relationship of the computational cell. Thus, terrain barriers that are not aligned with

cell faces will be missed in terms of their blocking ability which will result in an effect that, from now on, will be referred to as "leakage". To get around this problem, breaklines can be used to force the alignment of computational cell faces along with barriers or other features that will significantly affect the flow situation (Figure 3.2).

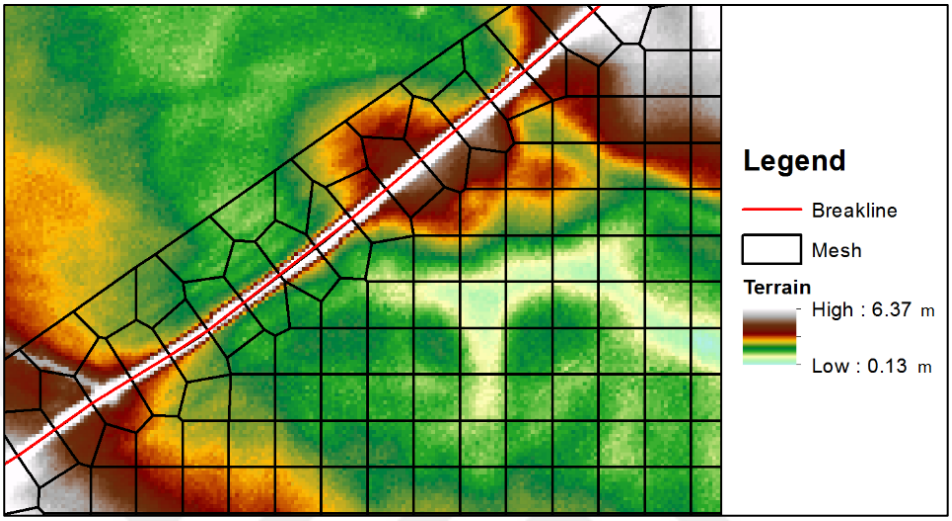

Figure 3.2. Illustration of a computational mesh with cells and a breakline

3.6.3. Hydraulic Structures

Modeling structures in 2D are not as well developed and researched as in the 1D case. Weirs, culverts, and gates can be added inside the 2D mesh and are modeled in 1D using the same equations as for the 1D case. No extra attention has to be added to cross section spacing and ineffective flow areas: the 2D equations will handle flow contraction and separation as long as the full momentum equations are used, and ineffective flow areas are considered as long as cell faces are aligned with the top of bridges and other barriers (USACE, 2016).

Bridges can be incorporated by modifying the terrain to capture bathymetry and banks underneath the bridge. However, this option cannot incorporate the bridge deck, meaning that it will fail to restrict the flow when the water surface reaches the bottom of the bridge deck. A more detailed representation of bridges can instead be done by expressing them as either culverts or gates. Using these options will likely require

additional work during calibration since little reference with respect to reasonable parameter values is found. In addition, the geometry of bridge openings is often hard to capture using culverts and gates (USACE, 2016).

3.6.4. Boundary Conditions

The same external boundary conditions that were presented in 1D (Flow hydrograph, stage hydrograph, rating curve, and normal depth) can be used in 2D. In addition, precipitation can also be an internal boundary condition.

In 2D, internal boundary conditions are set-up as boundary condition lines which are connected to one or more cells through the cell face points. With the exception of precipitation, boundary conditions can only be put at the perimeter of the mesh and not inside the mesh.

3.7. Two-Dimensional Hydraulic Computations

The 2D solver in HEC-RAS can compute water surfaces, flows and velocities using either the full momentum equations or the diffusive wave simplification. Each cell in the computational mesh makes up a control volume for which the water surface elevation and flow across the faces are to be solved. Integrating the continuity equation and rewriting using Gauss divergence theorem yields the following integral form of the continuity equation:

$$\frac{\delta}{\delta t}\iiint_{\Omega} d\Omega + \iint_{S} V \cdot n dS + Q = 0 \qquad (3.9)$$

Where Ω is the volume occupied by the fluid in the cell, S the cell boundary surface, n is normal to the boundary surface and Q is the volume flux from external sources. This equation can be discretized in a way that incorporates the available sub-grid information:

$$\frac{\Omega(H^{n+1}) - \Omega(H^{n})}{\delta t} + \sum_{k} V_k \cdot n_k A_k(H) + Q = 0 \qquad (3.10)$$

Where $\Omega(H)$ is a function describing the cell volume as a function of the water surface elevation, and $A_k(H)$ is a function of how the area of the cell face k varies with water surface elevation. The summation in the second term of equation 3.11 is over the faces of the cell. This form of the continuity equation can be combined with the simplified form of the momentum equation to obtain a new formulation of the diffusive wave equation, or it can be solved together with the full momentum equations (Betsholtz & Nordlöf, 2017).

3.8. Mapping

The most important step of the hydraulic modeling procedure is mapping. The required DEMs for the Wami River and Düden River were created from the elevation data obtained from the field studies at the project site.

Digital Elevation Models (DEMs) are a type of raster geographic information system (GIS) layer. In a DEM, each cell of the raster GIS layer has a value corresponding to its elevation (z-values at regularly spaced intervals). DEM data files contain the elevation of the terrain over a specified area, usually at a fixed grid interval over the "Bare Earth" (Figure 3.3). The intervals between each of the grid points will always be referenced to some geographical coordinate system (latitude and longitude or UTM (Universal Transverse Mercator) coordinate systems (Easting and Northing). For more detailed the information in DEM data file, it is necessary that grid points are closer together. The details of the peaks and valleys in the terrain will be better modeled with small grid spacing than when the grid intervals are very large (Colgan & Ludwig, 2016).

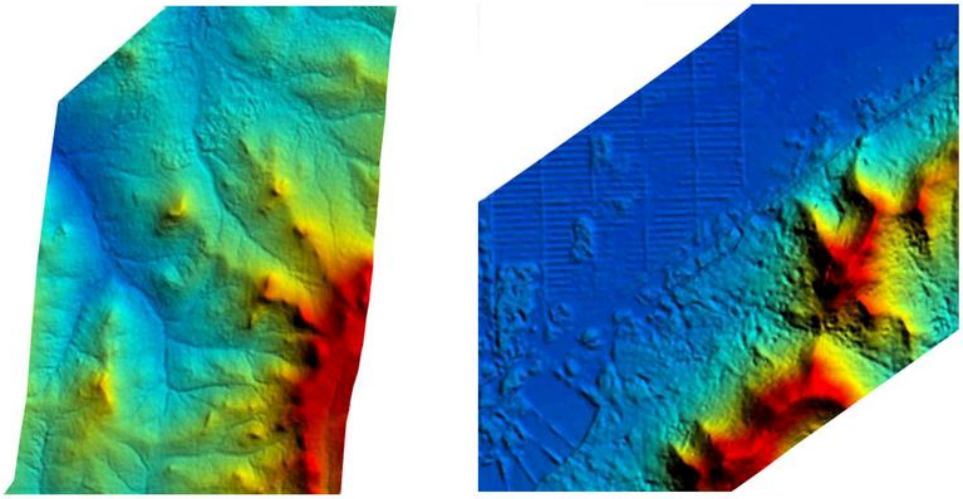

Figure 3.3. Digital Surface Model (DSM) for 5 Km Wide Pipeline Corridor

There is a variety of DEM source data available for developed areas and the suitability of this available data is depending on the project specifications. In remote regions around the World, were little or no source Data is available, the DEM can be produced by automatic DEM extraction from stereo satellite scenes.

A digital terrain model (DTM) can be described as a 3-dimensional representation of a terrain surface consisting of X, Y, Z coordinates stored in digital form (Figure 3.4). It includes not only heights and elevations but other geographical elements and natural features such as rivers, ridgelines, etc. A DTM is effectively a DEM that has been augmented by elements such as breaklines and observations other than the original data to correct for artifacts produced by using only the original data. With the increasing use of computers in engineering and the development of fast three-dimensional computer graphics, the DTM is becoming a powerful tool for a great number of applications in the earth and the engineering sciences (Colgan & Ludwig, 2016).

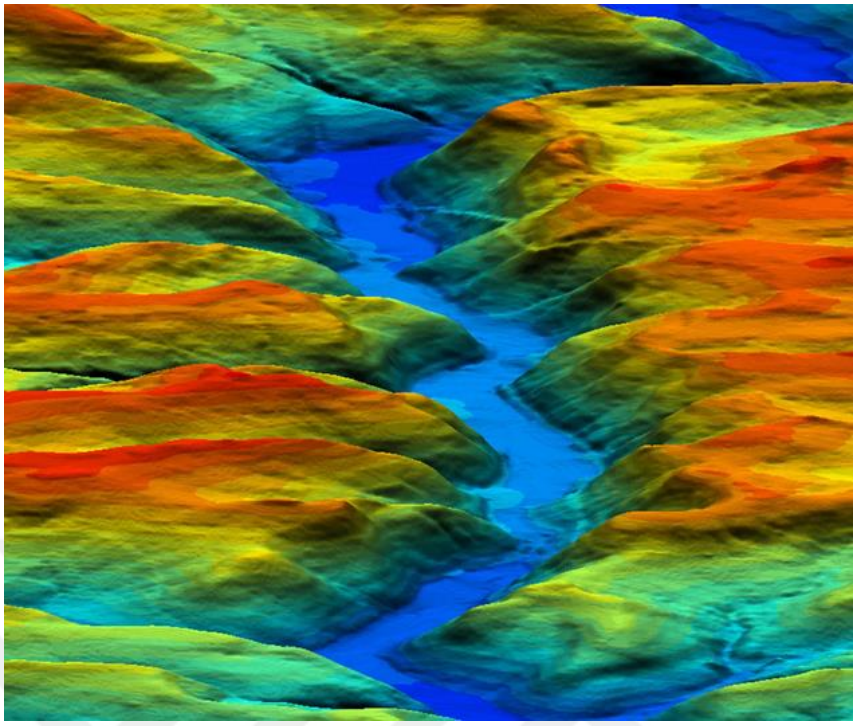

Figure 3.4. Digital Elevation Model

Digital Surface Model (DSM) represents the elevations of the reflective surfaces of trees, buildings, and other features elevated above the earth represents the surface and includes all objects on it. The difference between DEM/DTM and DSM can be seen in Figure 3.5 (Colgan & Ludwig, 2016).

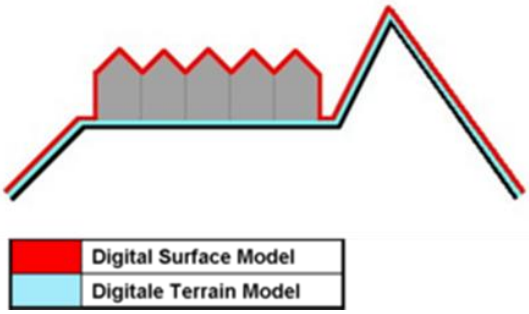

Figure 3.5. The difference between DTM (blue line) and DSM (red line) (Colgan & Ludwig, 2016).

Digital elevation data for Düden River was obtained from existing available data from the related governmental organizations, DSİ (State Hydraulic Works). 1/5000 scaled data were used for modeling areas. For the Wami River study, the topographic datasets

were provided by the Yapı Merkezi, which was the employer of the Railway Project. The topographic data sets were in point cloud form and are developed using Light Detection and Ranging Elevation Data (LiDAR) techniques. All the terrain models are used as sublayers for computational grids.

CHAPTER 4

WAMI RIVER

In this chapter, hydrological studies and modeling details of the Wami Bridge are described. The Standard Gauge Railway (SGR) is to be constructed between Morogoro-Dodoma-Makutupora (MDM) in Tanzania. Within the scope of the study; the first objective was to calculate the design discharge value for a 100-year return period for the hydraulic structure, Wami Bridge, which was named as BR01 in the simulations, along the proposed railway line. The general view of the railway line can be seen in Figure 4.1 where the bridge location is shown with a red arrow between Morogoro and Kilosa.

Figure 4.1. General view of Morogoro-Makutupora Railway Line

The United Republic of Tanzania borders Kenya and Uganda to the north; Rwanda, Burundi, and the Democratic Republic of the Congo to the west; Zambia, Malawi, and Mozambique to the south; and the Indian Ocean to the east. The Tanzanian mainland is divided into several clearly defined climatic regions: the coastal plains, which vary in width from 16 to 64 km and have lush, tropical vegetation; the Masai Steppe in the north, 213 to 1067 m above sea level, which gives rise to two prominent mountains, Kilimanjaro, 5895 m above sea level and Africa's highest peak, and Mount Meru, 4565 m; and there's a high plateau known as the Southern Highlands in the southern area towards Zambia and Lake Malawi.

There are four main climatic zones in Tanzania: (1) the coastal area and immediate hinterland, where conditions are tropical, with temperatures averaging about 27° C, rainfall varying from 1000 mm to 1930 mm, and high humidity; (2) the central plateau, which is hot and dry, with rainfall from 500 mm to 760 mm, although with considerable daily and seasonal temperature variations; (3) the semi temperate highland areas, where the climate is healthy and bracing; and (4) the high, moist lake regions.

As can be seen in Figure 4.2, the project area lies mostly in dry and moderate climate zones. There are average annual total rainfall values of Dodoma and Morogoro, which are the most important settlements within the project area, are 582 mm and 806 mm, respectively.

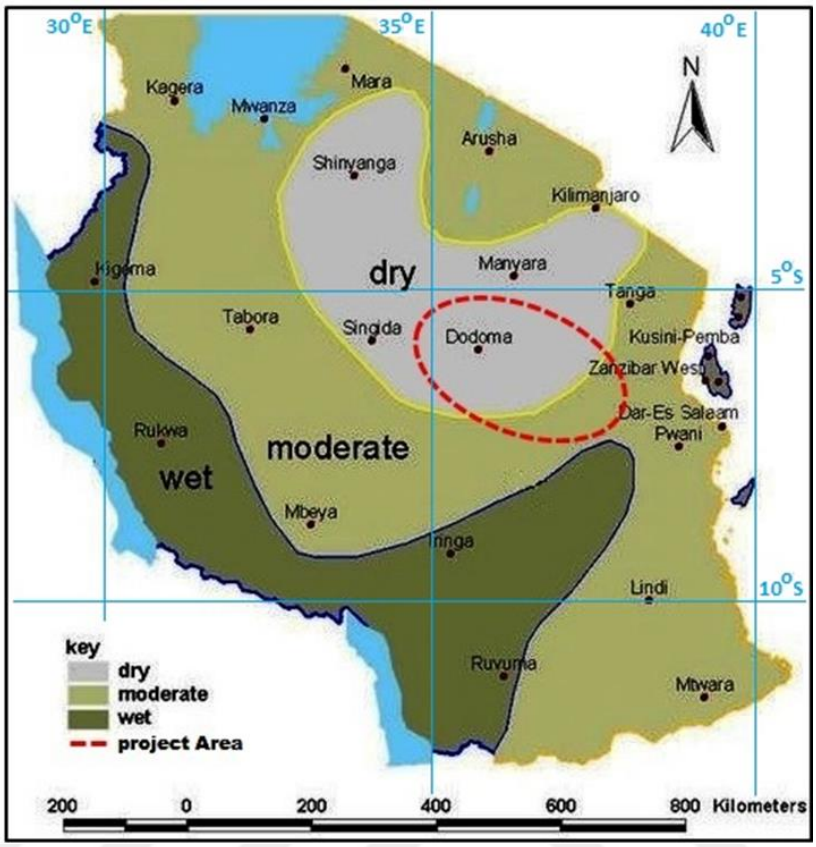

Figure 4.2. Climatic zone map of Tanzania (Fiddes, 1976)

The railway line is approximately 333 km long and is located within Ruvu Basin, Wami Basin, and Internal Basin. The main basins in Tanzania and the locations of the basins in which the project site is located are given in Figure 4.3.

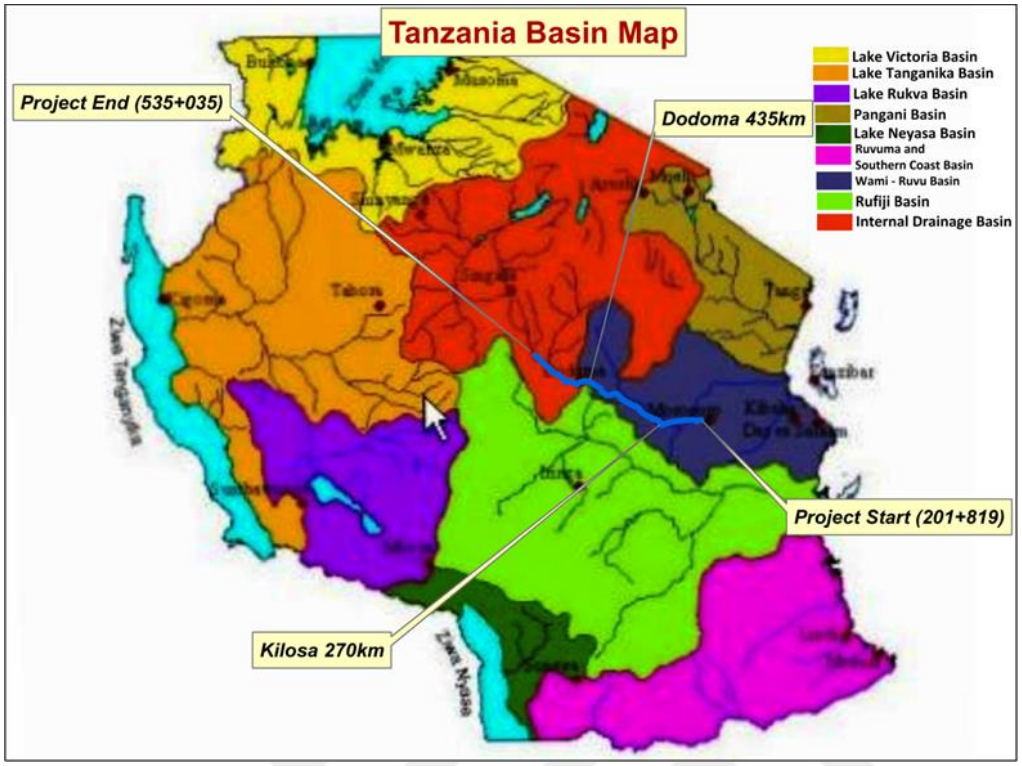

Figure 4.3. Main river basins in Tanzania

In the railway project designed, the digital elevation models of the BR01 bridge location are shown in Figure 4.4 and Figure 4.5. The SGR bridge crossing is located at chainage 216+888 and there is an existing railway under operation that is downstream of the planned MDM railway bridge. The bridge with a steel beam found on the existing railway is named as Cur_BR01 in the study.

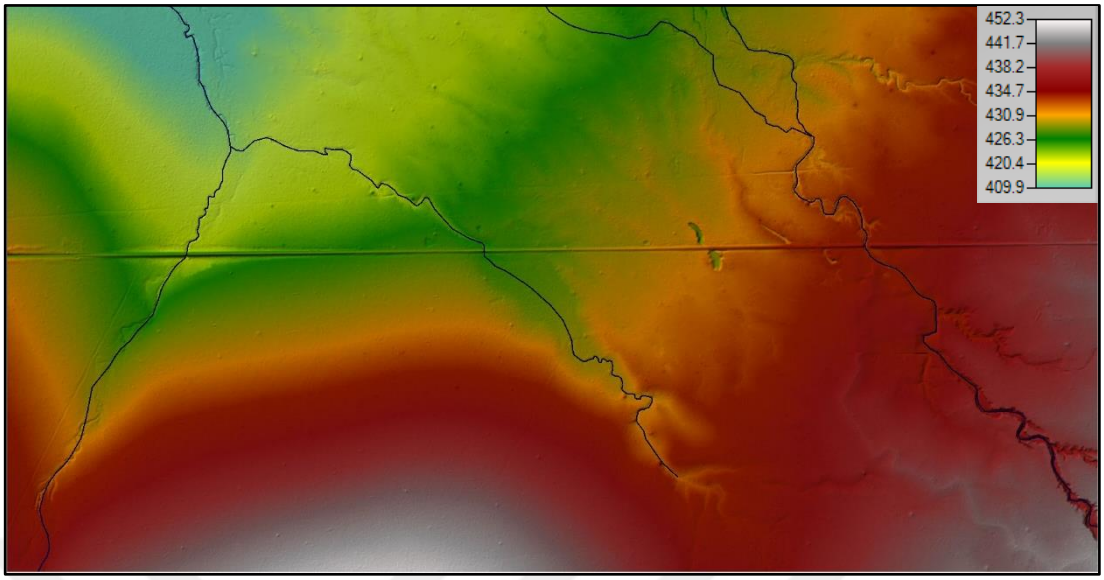

Figure 4.4. Existing case digital elevation model (scale 1:250000)

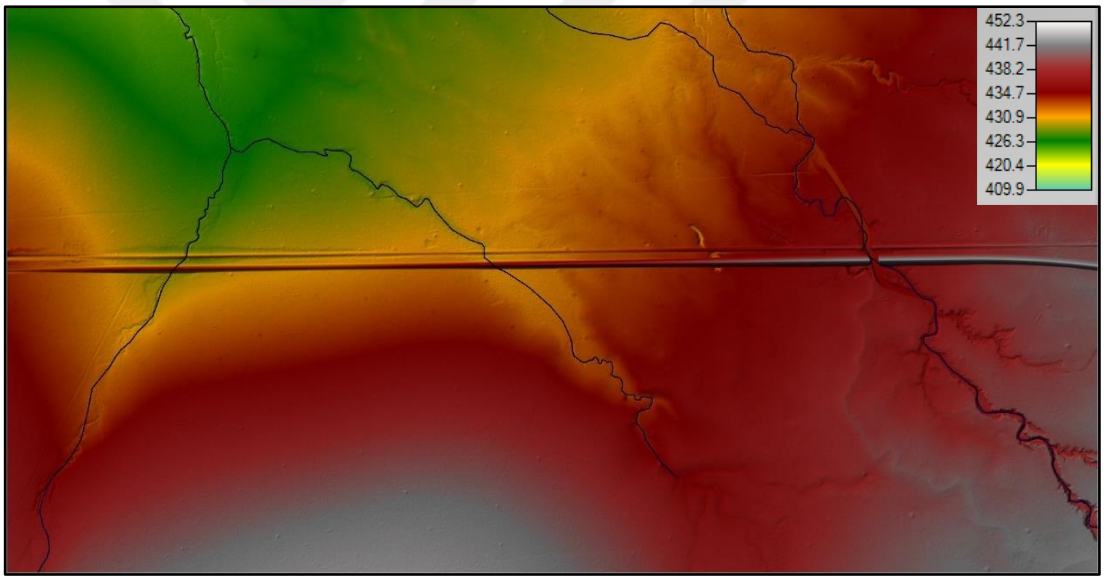

Figure 4.5. Design case digital elevation model (scale 1:250000)

In addition to the bridge, two culvert crossings (at chainage 217+876 and 218+670) were added to this model since the influence of the overflooding from the bridge affects these two culverts. Since the topography is extremely flat and so that there are flow transitions between the basins, it is the right way to incorporate existing culverts into the evaluation for the BR01 bridge and solve all these hydraulic structures as a

system. The flow passing through the neighboring basins from the left bank of the BR01 bridge is considered thus the capacities of the culverts at km 217+876 and km 218+670 are evaluated realistically.

The distance between the start and the end of the stream which BR01 bridge is located is approximately 3000 m. This distance determines the length of the computational grid used in the calculations, while the predicted flood area determines the width of this domain, which is approximately 2200 m. The modeling area which covers three different streams is about 529 ha.

100-year return period hydrographs calculated for bridges BR01, culverts at 217+874 and km 218+670 (with areas of 55.22 km^2, 8.23 km^2, and 3.29 km^2 respectively), have been used as the upstream boundary condition for each river. For the downstream boundary condition, the 0.004 value of the riverbed slope is used. The outer boundaries are chosen as far away as possible from the project area to remove the faults that could be caused by upstream and downstream boundary conditions. Thus, even if the boundary condition is not precisely defined, errors on the water surface level are eliminated by the iterative backwater calculation method and water surface profile converges to the same level at the project area.

The existing situation is examined to evaluate possible flood risks of the BR01 bridge located at km 216+868. Subsequently, the vertical profile of the designed SGR designed embankment is embedded into the existing digital elevation model with the help of the "connection editor" as a weir. In this weir representing the MDM railway, the culverts are placed where the stream passes, and the model is analyzed for design case.

The two-dimensional analysis was performed using this new model geometry. Thus, it is determined how the designed railway project affected the flood inundation area and whether the opening size of the designed and existing drainage structures are sufficient or not. It is also determined through this flood model whether the maximum water surface elevation at the upstream of railway embankment causes any

overflooding or adequate to the design criteria. Presented in the following sections are geometry data, land use classifications in terms of the Manning's n value, and flow data for 100-year return period flood hydrographs.

4.1. Geometric Data

In this part of the project, there is an existing railway line still under operation at the downstream of the SGR designed route. The existing steel beam bridge named as Cur_Br01, with an opening size of 15m span and less than 1m opening height partially blocked by sediment accumulation as shown in the figure below. Due to the accumulation of sediment upstream of the bridge, the opening of the bridge is reduced significantly. As can be seen from the photographs given in Figure 4.6 and Figure 4.7, the right side of the bridge is almost completely closed. This situation has been taken into consideration when modeling the bridge section.

Figure 4.6. The upstream side of the existing bridge (Cur_BR01)

Figure 4.7. The downstream side of the existing bridge “Cur_BR01”

In addition, the culverts on the existing railway are added into the models. After the addition of the existing hydraulic structures, the grille with the "Conspan-arc" geometry is defined for the BR01 bridge for the SGR designed. Subsequently, existing rectangular cross-section culvert defined at km 217+874 and existing arch culvert at km 218+670 are included in the model. The locations of existing and designed hydraulic structures are shown in Figure 4.8.

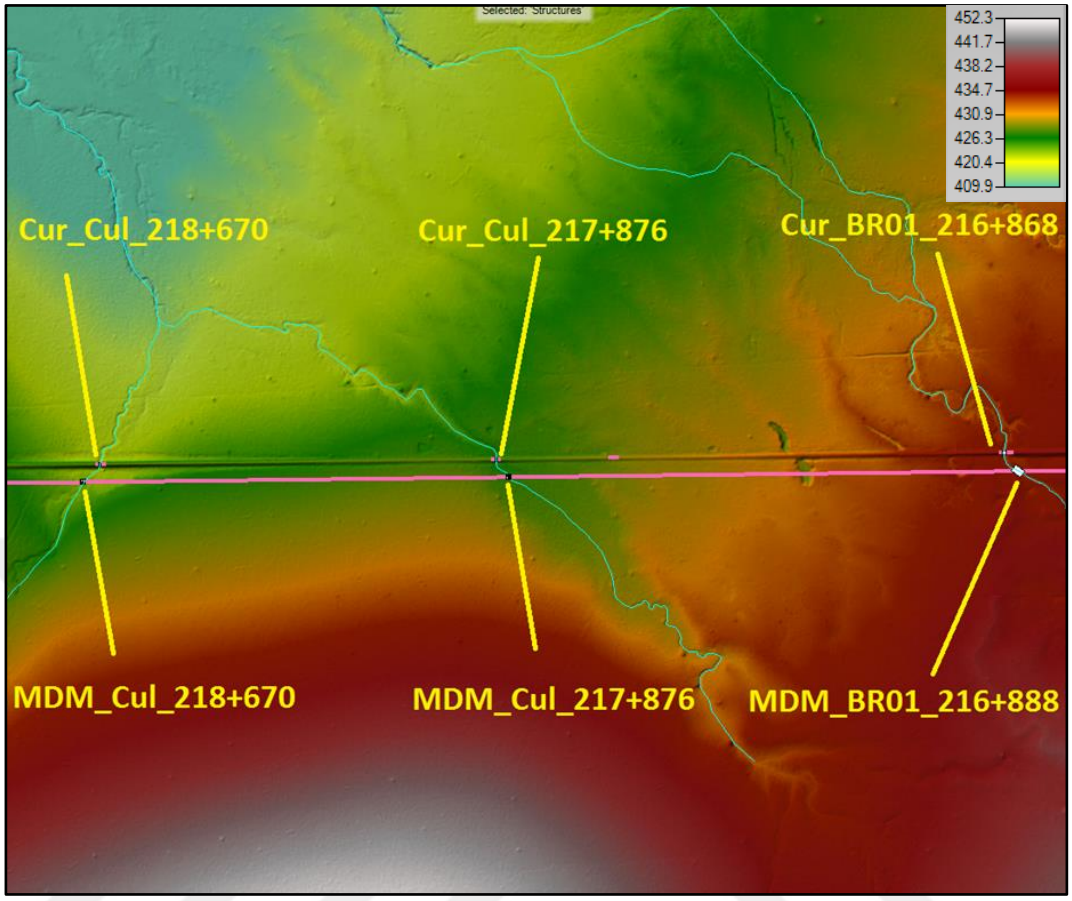

Figure 4.8. Layouts of hydraulic structures with existing and designed railways

The hydraulic cross-sections of the three existing structures that entered to the geometric data editor are given in Figure 4.9. For the existing BR01 bridge, an opening of 7.0 m width and 1.0 m height is defined to the left side of the cross-section. From the site investigations, the unfilled bridge opening was identified as 15-m width and 2-m height. The dimensions of the existing culverts are 2.00 m x 1.30 m for km 217+874 and 2.00 m x 1.60 m for km 218+670.

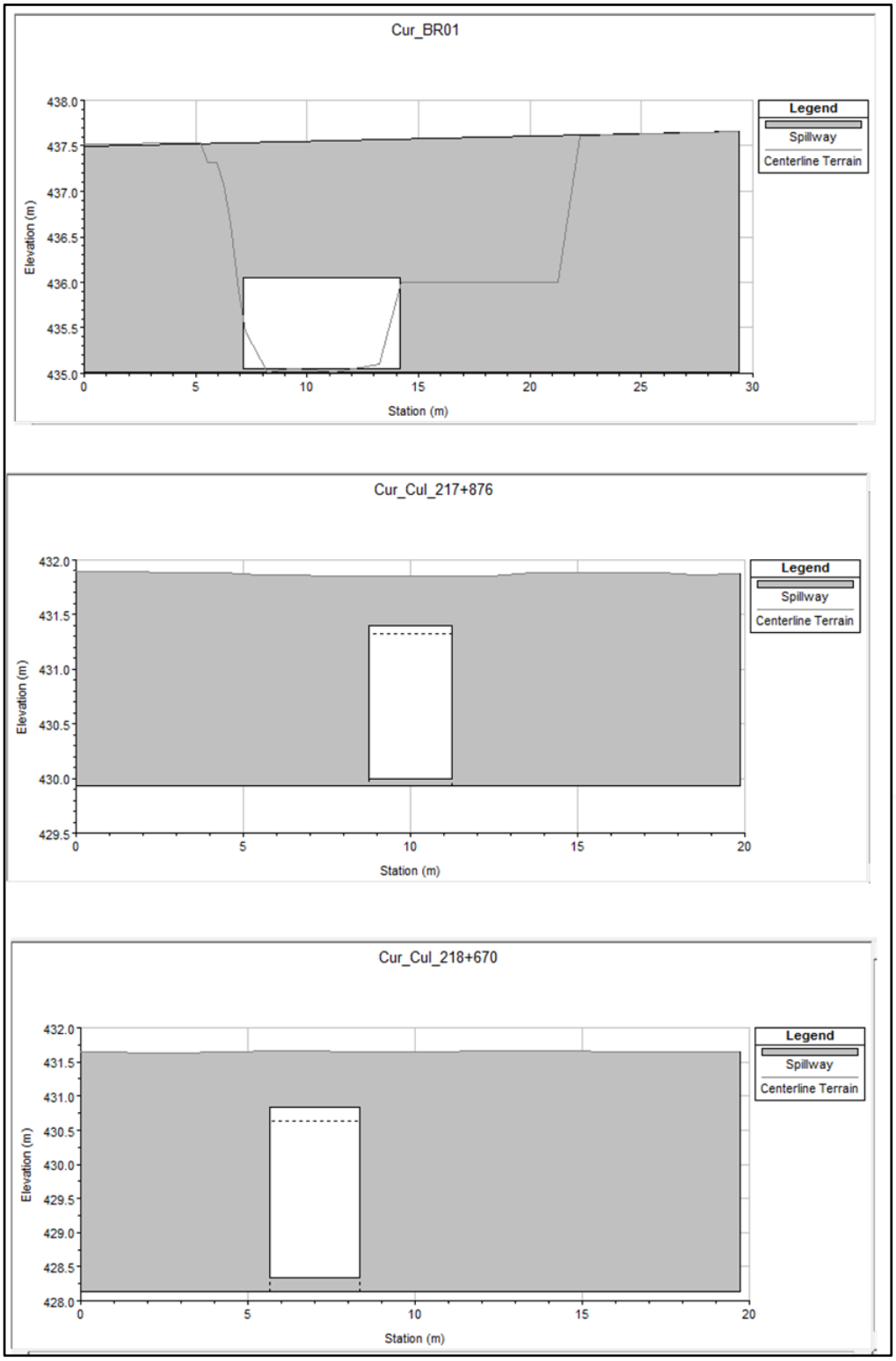

Figure 4.9. Sections of the existing hydraulic structures

The vertical profile of the MDM railway and the locations of the hydraulic structures designed on it are given in Figure 4.10.

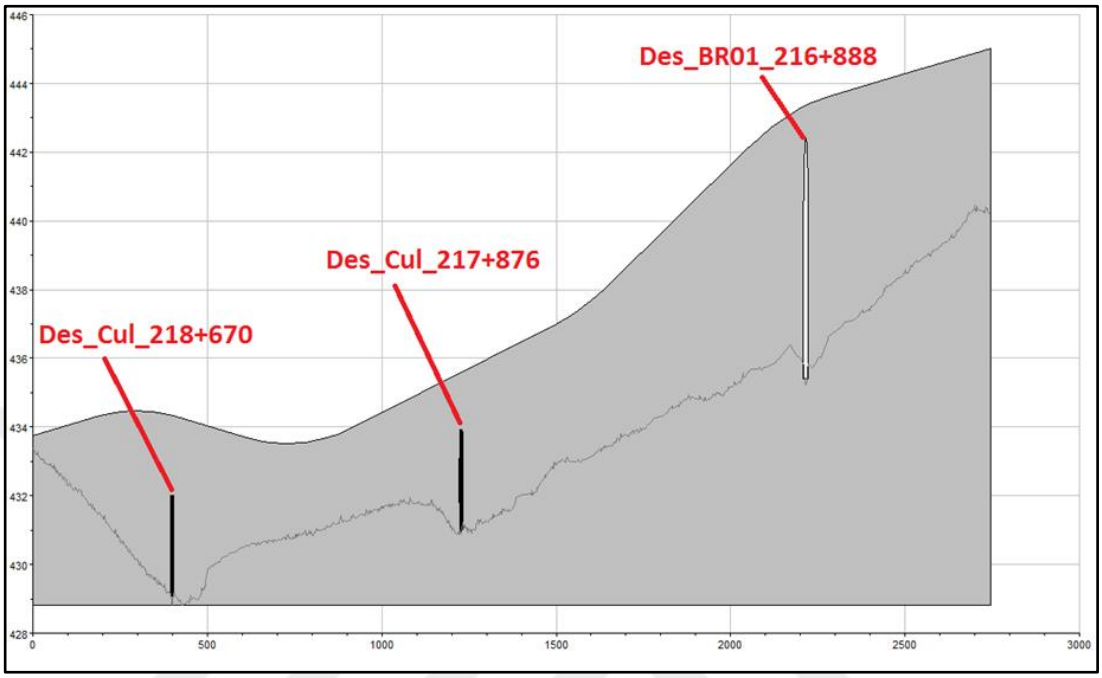

Figure 4.10. MDM railway profile and location of the hydraulic structures

The section designed for the BR01 has a width of 15.0 m and a height of 7.0 m with an arc roof culvert. Inlet and outlet invert elevations of culvert are both 434.5 m.

The culvert at km 217+876 has 1 barrel which is 2.94 m diameter. The inlet and outlet elevations are 430.90 m and 430.85 m, respectively.

The culvert at km 218 + 670 has 2 barrels with 2.94 m diameter each. The inlet and outlet elevations are 428.90 m and 428.85 m, respectively. All hydraulic structure sections on the MDM railway are shown in Figure 4.11.

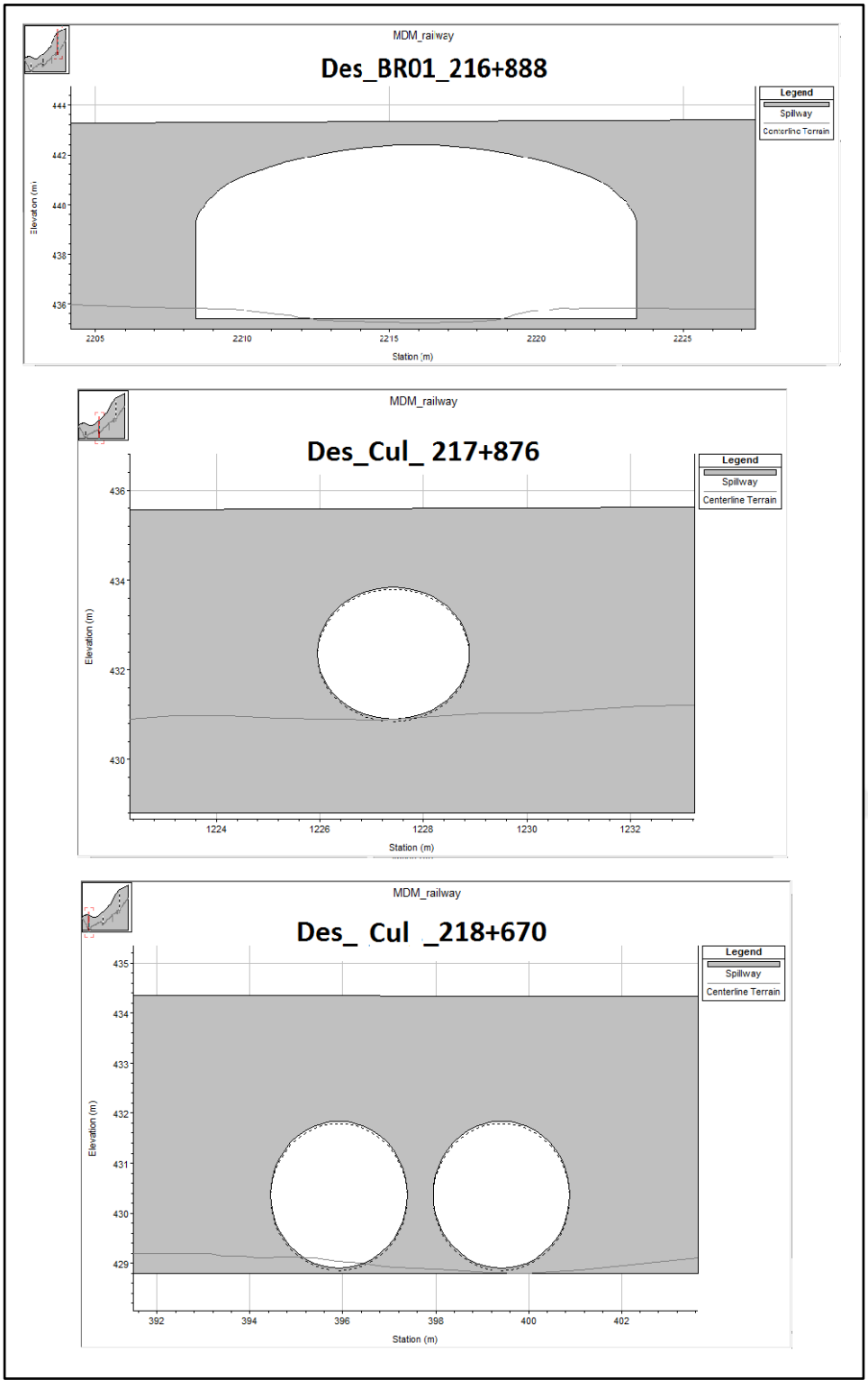

Figure 4.11. Sections of designed hydraulic structures

After adding bridges and culverts, a 2D computational grid was created. For the preliminary computations, the cell size for the grid was selected to as 10x10 m. Subsequently, the cell dimensions are reduced to 2x2m from 10x10m, minimizing cell sides 1 m at a time to obtain a proper computational grid for the model to have realistic hydraulic behavior in the region.

In Figure 4.12, the computational grid with 3x3m cell sizes is given. This computational grid is used because of two reasons: first, the computations with 2x2m and 3x3m grids have almost the same flooding results (WSE and inundation area) and secondly the computation time is almost tripled when 2x2m grid is used instead of 3x3m.

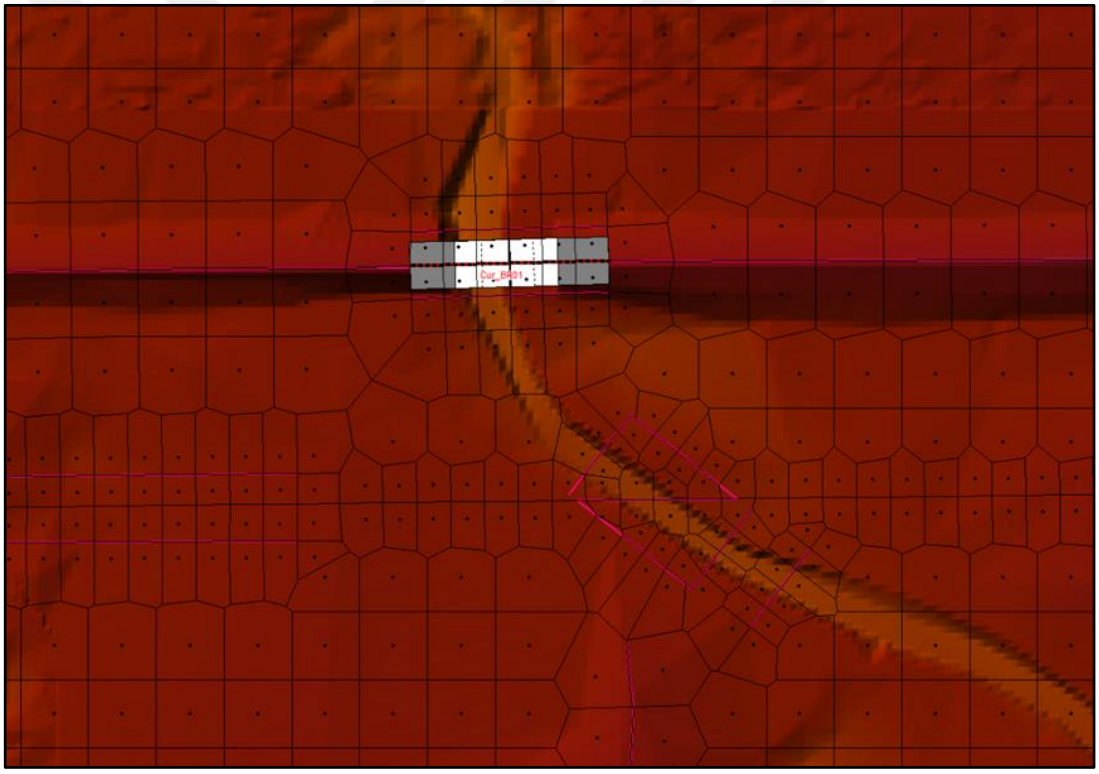

Figure 4.12. Part of the computational grid with different cell size (BR01 location)

HEC-RAS uses this underlying terrain to develop the geometric and hydraulic property (cross-sectional area, wetted perimeter, hydraulic radius and conveyance) tables that represent the cells and the cell faces. Once the cells are defined, the analysis is performed with the aid of the hydraulic property tables generated for each cell.

4.2. Flood Design Flow Rates

In order to estimate the design flood flow rates for the basins of the Tanzanian MDM railway project, the Transport Road Research Laboratory East African Flood Model method (TRRL EAFM) is used. It is a simple technique for estimating design hydrographs for ungauged catchments. In common with the unit hydrograph losses model, the method consists of converting a given design storm to runoff using an appropriate model. In both methods, it is assumed that a storm of a given return period will cause a flood of the same return period. The actual response of a catchment will depend on the local antecedent conditions and the assumption may not be strictly true, but in the absence of detailed local information it is reasonable (Fiddes, 1976).

A reservoir is said to be linear if the outflow (q) is related to the water stored in the reservoir by the linear relationship:

$$q = \left(\frac{1}{K}\right) S \qquad (3.11)$$

Where; S is the reservoir storage and K is the reservoir lag time.

The hydrograph peak factor (F) is given as 2.3 for lag time K>1 hour and 2.8 for K< 0.5 hours. This peak flow factor is defined as the ratio of peak flow Q_p and average flow Q_{avg} during the base time T_B, that is:

$$F = Q_p / Q_{avg} \qquad (3.12)$$

The selected design storm is converted to runoff using a simple three-parameter model, whose parameter values depend on the catchment's physical and climatological characteristics (Fiddes, 1976).

The calculation procedure of TRRL EAFM is explained as follows:

- Catchment Area, land slope and channel slope are measured for each catchment by the help of geographic information system tools.

- From site inspection reports and land cover maps, catchment type and lag time are established according to the table below. Lag time (K) for cultivated land and forest on the overgrown valleys is calculated as a weighted average according to field condition (Fiddes, 1976).

Table 4.1. *Catchment lag times (Fiddes, 1976)*

Catchment Type	Lag Time (K) hrs.
Arid	0.1
Very Steep Small Catchment	0.1
Semi-Arid Scrub (Large)	0.3
Poor Pasture	0.5
Good Pasture	1.5
Cultivated Land	3.0
Forest, Overgrown Valley	8.0
Papyrus Swamp in Valley	20.0

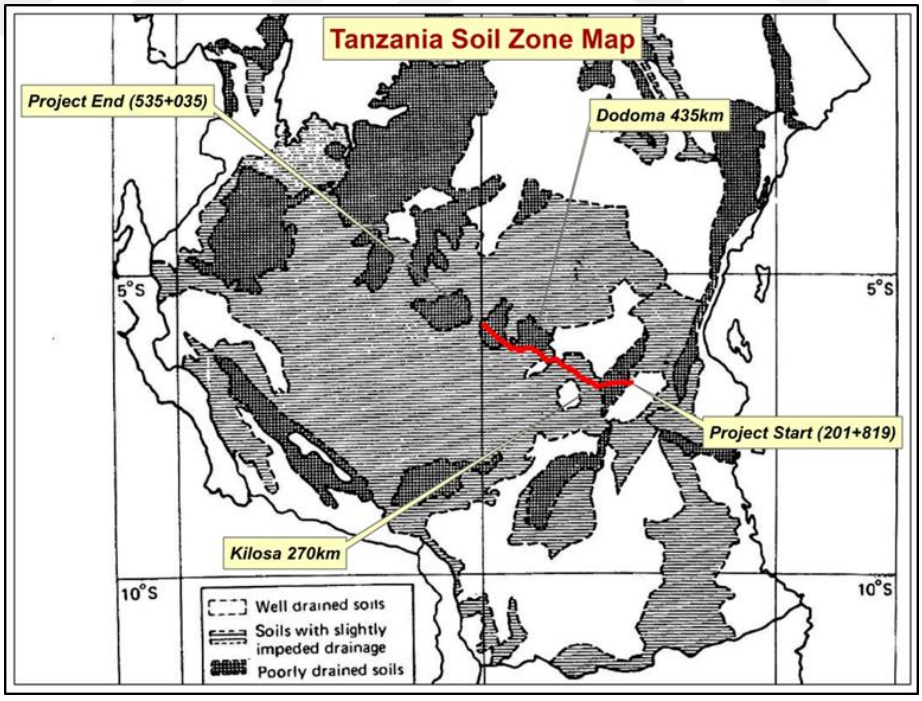

Figure 4.13. Soil zones in Tanzania map (Fiddes, 1976)

- With land slope information, the standard contributing area coefficient (Cs) is estimated for each catchment using the table below.

Table 4.2. *Standard contributing area coefficients (Fiddes, 1976)*

Catchment Slope	Soil Type		
	Well Drained	Slightly Impeded Drainage	Impeded Drainage
Very Flat < 1.0%	-	0.15	0.30
Moderate 1-4%	0.09	0.38	0.40
Rolling 4-10%	0.10	0.45	0.50
Hilly 10-20%	0.11	0.50	-
Mountainous >20%	0.12	-	-

- The study area is in the Central Tanzania region which is an area of dry and semi-arid zones. The stream is taken as seasonal and thus C_W coefficient is taken as 1.0 in the study.

Table 4.3. *Catchment wetness factor (Fiddes, 1976)*

Rainfall Zone	Catchment Wetness Factor	
	Perennial Streams	Ephemeral Streams
Wet Zones	1.0	1.0
Semi-Arid Zone	1.0	1.0
Dry Zones	0.75	0.50
West Uganda	0.60	0.30

- From site inspection reports and land cover maps, the vegetative cover is determined. Since the antecedent rainfall zone above is accepted as dry zone, initial retention, Y, is taken as zero.
- From Figure 4.14, the study area is found to be within Inland Zone. Tp and n values of the bridge area are equal to 0.96 and 0.75 respectively for the Inland zone (Table 4.4).

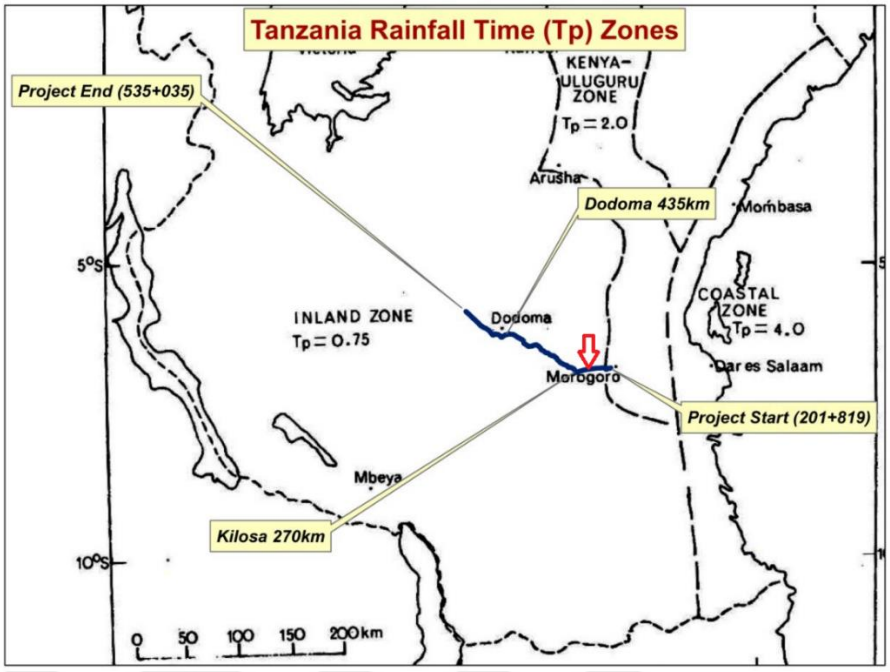

Figure 4.14. Rainfall time (Tp) zones (Fiddes, 1976)

Table 4.4. *Rainfall time for East African Storms (Fiddes, 1976)*

Zone	Index (n)	Rainfall Time (T_P) (hour)
Inland Zone	0.96	0.75
Coastal Zone	0.76	4.0
Kenya-Uluguru Zone	0.85	2.0

- Design storm rainfall value catchment during a time interval (T_B) is calculated using the formula:

$$R_{TB-T} = \frac{T_B}{24}\left(\frac{24.33}{T_B} + 0.33\right)^n * R^{T/24} \qquad (3.13)$$

- As $n = 0.96$ for the zone in which the project road lies. $R^{T/24}$ is the T year 24-hr storm rainfall. R_{TB-T} is design storm rainfall for T_B hours for T year return period.T_B, the base time:

$$T_B = Tp + 2.3K + T_A \qquad (3.14)$$

- Here, T_P is the time during which the rainfall intensity remains at a high level. T_R is the recession time for the surface flow estimated as T_R = 2.3K, (K; the time of lag). T_A is attenuation time of the flood wave:

$$T_A = 0.028 \frac{L}{Q_{avg}^{0.25} S^{0.5}} \quad (3.15)$$

where L is the stream length, Q_{avg} is the estimated average discharge and S is the average mainstream slope. Since TRRL EAFM has an iteration computational procedure, first T_A value is assumed, and, in this project, all initial T_A values are assumed to be 0 as a starting step (Fiddes, 1976).

- After obtaining R_{TB-T} as a point rainfall, using areal reduction factor for Tanzania, it has been reduced to areal rainfall:

$$P_T = R_{TB-T} ARF \quad (3.16)$$

Where, P_T is the T-year areal rainfall during the base time T_B and for Tanzania, ARF is determined using the equation:

$$ARF = 1.0 - (0.04 T_B^{-0.33} A^{0.5}) \quad (3.17)$$

Where A is the catchment area. Then, the total volume of runoff R_O is calculated:

$$R_O = 10^3 (P_T - Y) C_A A \quad (3.18)$$

Here, P_T is the total storm rainfall (mm) during a period equal to the base time T_B. Y is the initial retention in millimeters. C_A is the contribution area coefficient. A is the catchment area in square kilometers.

- For the hydrograph time base T_B, storm rainfall P and a total volume of runoff R_O, the average flow Q_{avg} is calculated:

$$Q_{avg} = 0.93 R_O / (3600 T_B) \quad (3.19)$$

Then finally, T_A is recalculated using the formula:

$$T_A = 0.028L/(Q_{avg}^{0.25}S^{0.5}) \quad (3.20)$$

After calculating T_A, last steps are iterated until Q_{avg} is within 5% of the previous estimate.

- The final step is to calculate design discharge for T year return period. Here, hydrograph assumed has a peak factor as explained before.
- For a lag time $K > 1$ hour, F is given as 2.30 and for a lag time $K < 0.5$ hours, F is given as 2.80 (Equation 3.1).
- This peak flow factor is defined as the ratio of peak flow Q_P and average flow Q_{avg} during the base time T_B, which is given in equation 3.13:

The basin area calculated at section **BR01** located at Km 216+888 is **52.80 km²**. The 100-year return period flood peak value produced by this basin is **106.77 m³/s**. For the culverts located at km 217+874 and km 218+670, the basin areas were calculated as 8.25 km2 and 3.29 km2, respectively. For these basins, 100-year return period peak flow values are calculated as **62.23 m³/s** and **23.54 m³/s**, respectively. These values are used for both the existing state and the design state. It is assumed that the starting times are the same for all hydrographs and these three hydrographs are entered as upstream boundary conditions for each river.

4.3. Land Use and Roughness

The roughness parameter, Manning's n value, is an important parameter that can be used in calibrating the two-dimensional model. For the 2D model, RAS Mapper has the ability to create a land cover layer and associate this layer with terrain data. RAS Mapper also allows modelers to specify manning's roughness values with various land use categories that, in turn, are defined in the land cover layer. The end result of this is that RAS Mapper will associate a Manning's roughness value with each computational cell faces.

HEC-RAS uses Manning's formula to compute friction along the ground surface. Friction losses are used in the solution methodology employed by HEC-RAS, in particular, the Conservation of Momentum equation.

Land use classes for the two-dimensional model were determined using on-site observations and aerial photographs. In the flood inundation region, there are generally woody and bushy areas with different densities close to the rivers. In areas far from the rivers, poor vegetation or pasture areas have been observed. There is no dwelling area in the area. The manning roughness values used according to the land classes determined for the project area are given in Figure 4.15.

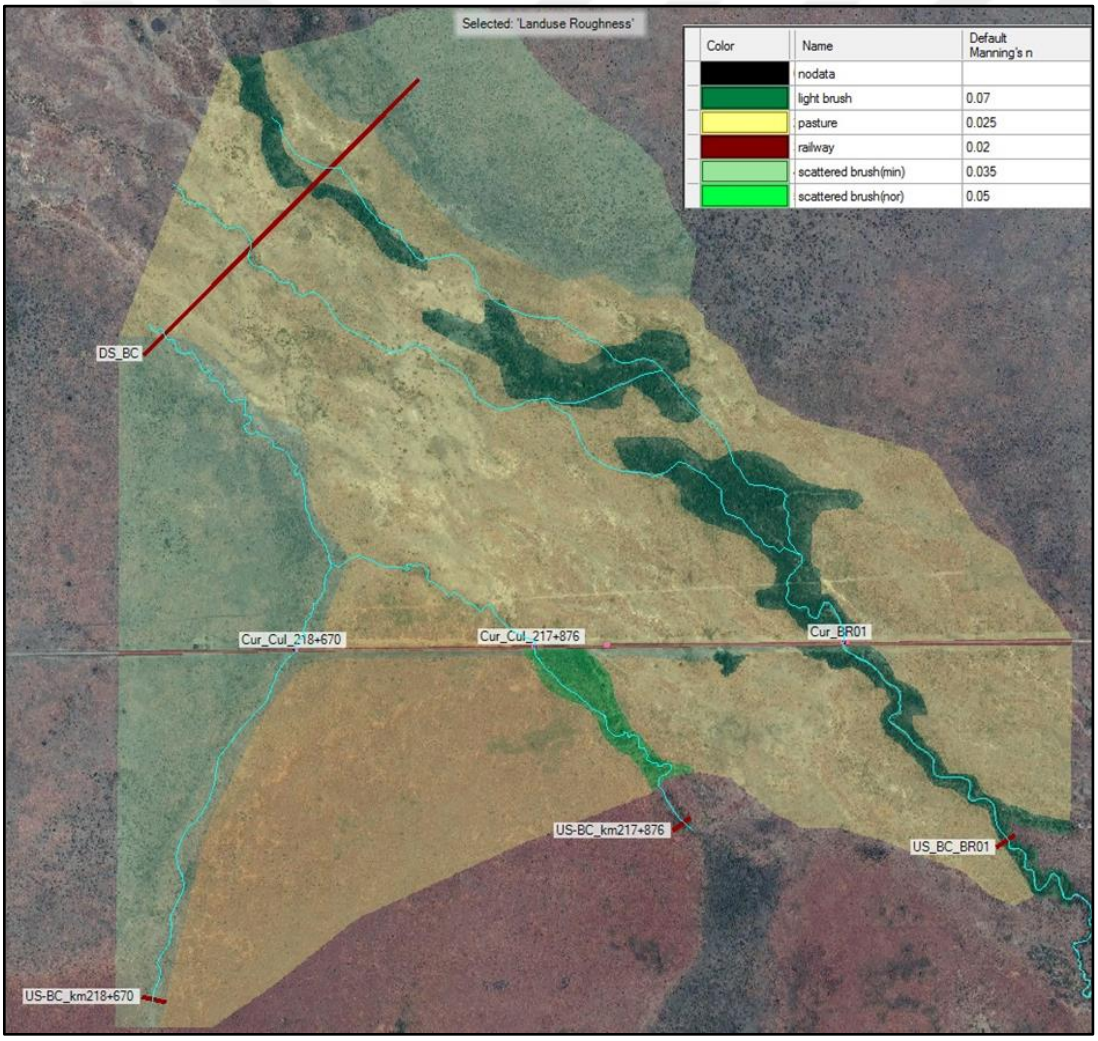

Figure 4.15. Manning's 'n' values plan view

The two-dimensional roughness map, which defines the conveyance value, of each cell face in the grid is given in Figure 4.16. Manning roughness is defined as 0.070 in regions with "light to dense brush" as seen, but this value is defined as 0.025 for poor-vegetated regions around. The roughness value on the existing railway is accepted as 0.020.

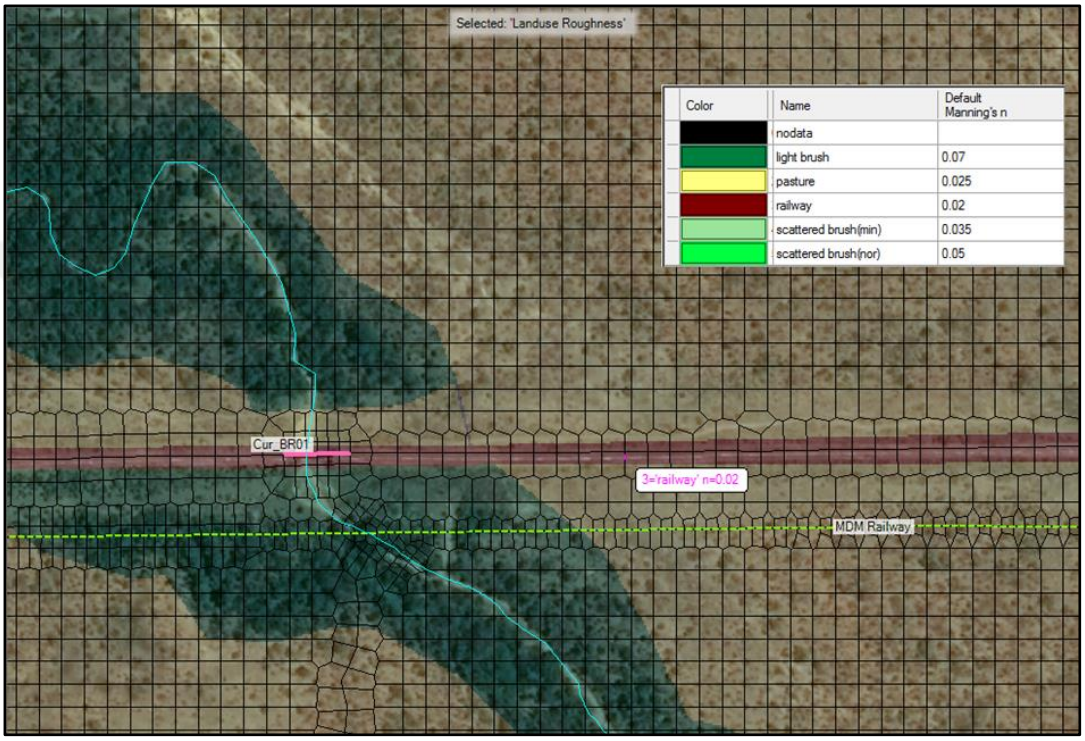

Figure 4.16. Manning's 'n' values for the project area plan

Roughness values assigned to terrain classes are taken from the HEC-RAS Hydraulic Reference Manual and are given in Table 4.5.

Table 4.5. *Manning's 'n' values (Open Channel Hydraulics, Chow, 1959)*

Type of Channel and Description	Minimum	Normal	Maximum
A. *Natural Streams*			
1. **Main Channels**			
a. Clean, straight, full, no rifts or deep pools	0.025	0.030	0.033
b. Same as above, but more stones and weeds	0.030	0.035	0.040
c. Clean, winding, some pools and shoals	0.033	0.040	0.045
d. Same as above, but some weeds and stones	0.035	0.045	0.050
e. Same as above, lower stages, more ineffective slopes and sections	0.040	0.048	0.055
f. Same as "d" but more stones	0.045	0.050	0.060
g. Sluggish reaches, weedy. deep pools	0.050	0.070	0.080
h. Very weedy reaches, deep pools, or floodways with heavy stands of timber and brush	0.070	0.100	0.150
2. **Flood Plains**			
a. Pasture no brush			
1. Short grass	0.025	0.030	0.035
2. High grass	0.030	0.035	0.050
b. Cultivated areas			
1. No crop	0.020	0.030	0.040
2. Mature row crops	0.025	0.035	0.045
3. Mature field crops	0.030	0.040	0.050
c. Brush			
1. Scattered brush, heavy weeds	0.035	0.050	0.070
2. Light brush and trees, in winter	0.035	0.050	0.060
3. Light brush and trees, in summer	0.040	0.060	0.080
4. Medium to dense brush, in winter	0.045	0.070	0.110
5. Medium to dense brush, in summer	0.070	0.100	0.160
d. Trees			
1. Cleared land with tree stumps, no sprouts	0.030	0.040	0.050
2. Same as above, but heavy sprouts	0.050	0.060	0.080
3. Heavy stand of timber, few down trees, little undergrowth, flow below branches	0.080	0.100	0.120
4. Same as above, but with flow into branches	0.100	0.120	0.160
5. Dense willows, summer, straight	0.110	0.150	0.200

4.4. Analysis

In the digital elevation model used in the analysis of the existing case, the newly designed railway line is not included. For the design case analysis, the newly designed railway line is added in the model parallelly to the existing railway. These conditions were given in Figure 4.4 and Figure 4.5.

4.4.1. Analysis of Current Situation

Two-dimensional hydrodynamic analyses have been carried out for the present situation using the above-described terrain model and boundary conditions. First, the resulted maximum water depths and flood inundation area of the existing situation are shown in Figure 4.17 on both the digital elevation model and aerial photo.

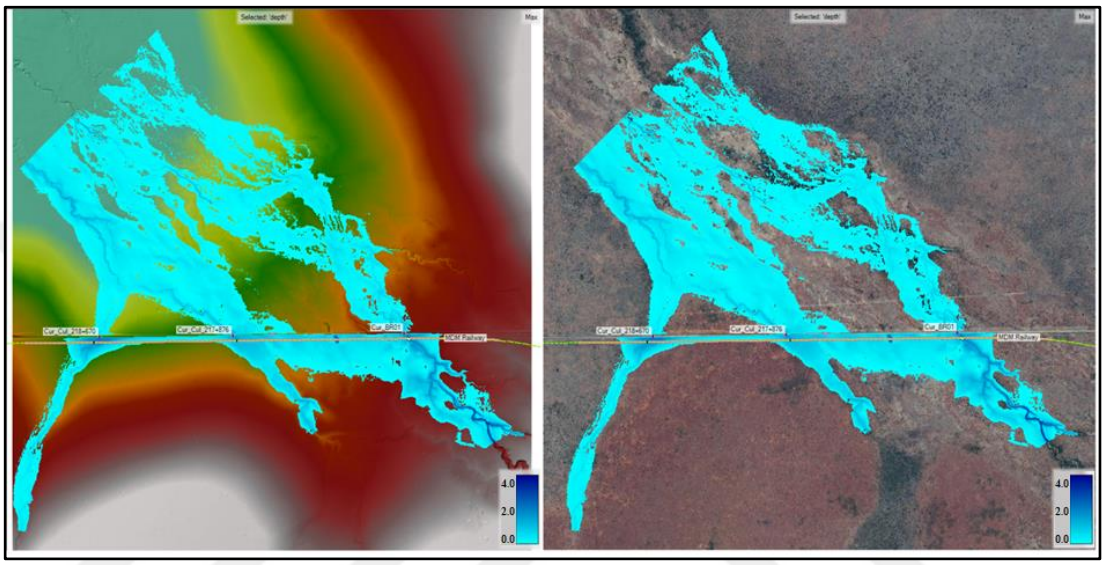

Figure 4.17. The depth map on DTM and aerial photo for the existing case (m)

At the beginning of the simulation, overtopping occurs on the left bank of the river just upstream of the current BR01 bridge.

A water surface profile and direction of the velocity vectors are taken from the section where the overtopping takes place is given in Figure 4.18. As the simulation progresses and the inflow values rise, the overflow occurs along the orange line. Since the existing Cur_BR01 bridge is filled leaving and 7.0 x 1.0 m opening (the original dimension was 15.0 x 2.0 m), the lowered hydraulic capacity causes swelling and spreading to the adjacent basins.

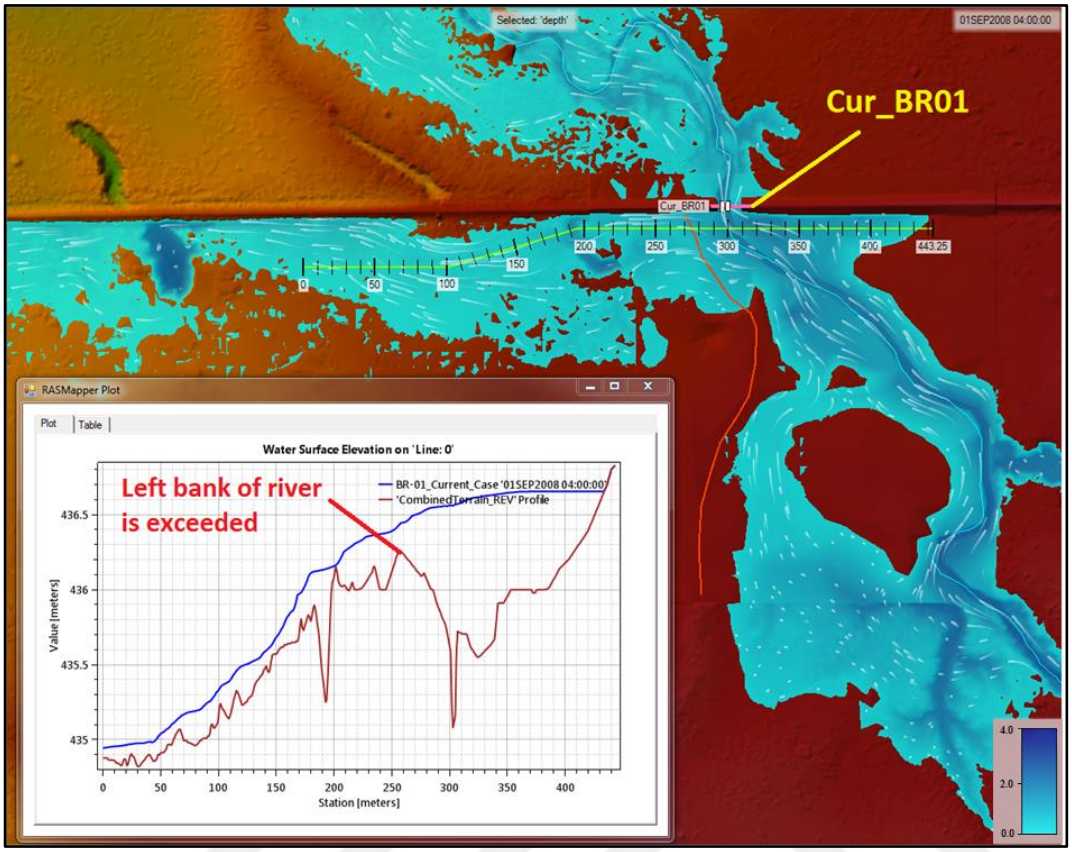

Figure 4.18. Location of river overtopping at Cur_BR01; water depth map (m)

The flows that over flooded the river left bank leads towards the culverts on the left side and are drained by these culverts. However, the capacities of existing culverts exceeded by additional flows and are overtopping occurs at the existing railway. In the section where Cur_Cul_217+876 is located, the overflows can be seen in Figure 4.19. In this section, as seen from the profile, the water level above the railway fill is about 30 cm. There is no overflow on the existing railway except this region.

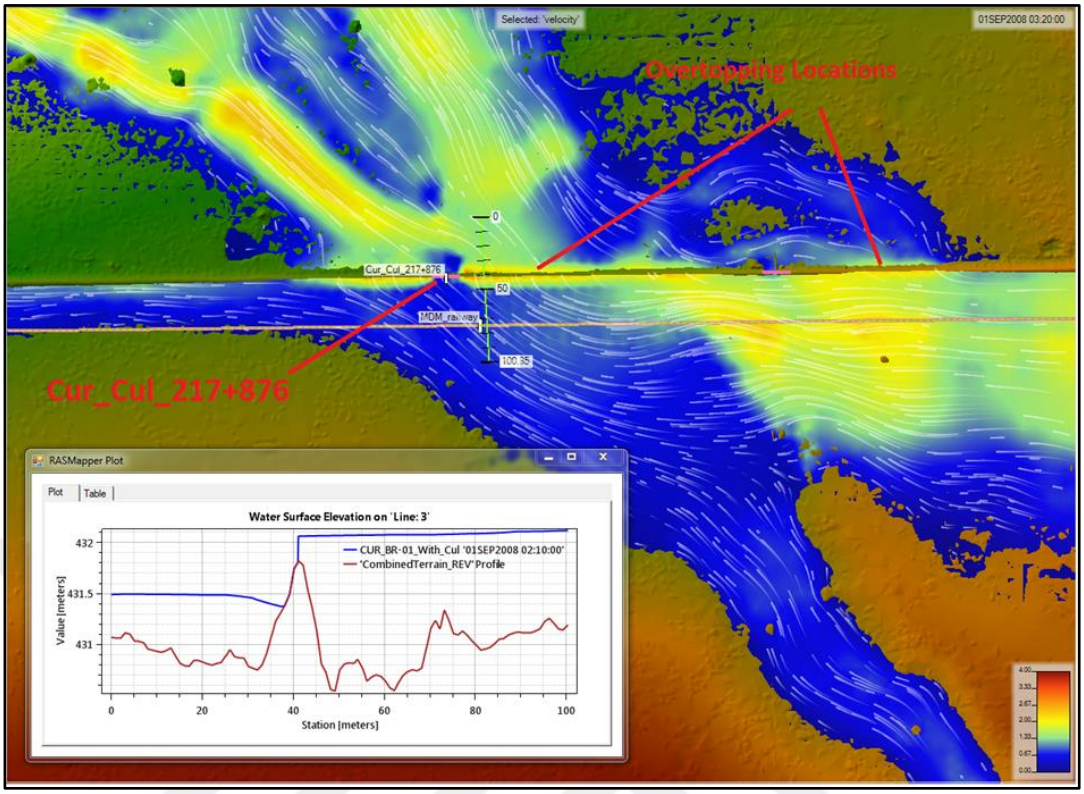

Figure 4.19. Overtopping observed close to Cur_Cul_217+876

The graphs showing the discharge capacities of the culverts and bridge over the existing railway during the simulation are given in Figure 4.20. According to this, Cur_Cul_217+876 culverts seem to be overflowing. The maximum flow values of structures are 20.40 m^3/s, 9.64 m^3/s, and 14.02 m^3/s, respectively.

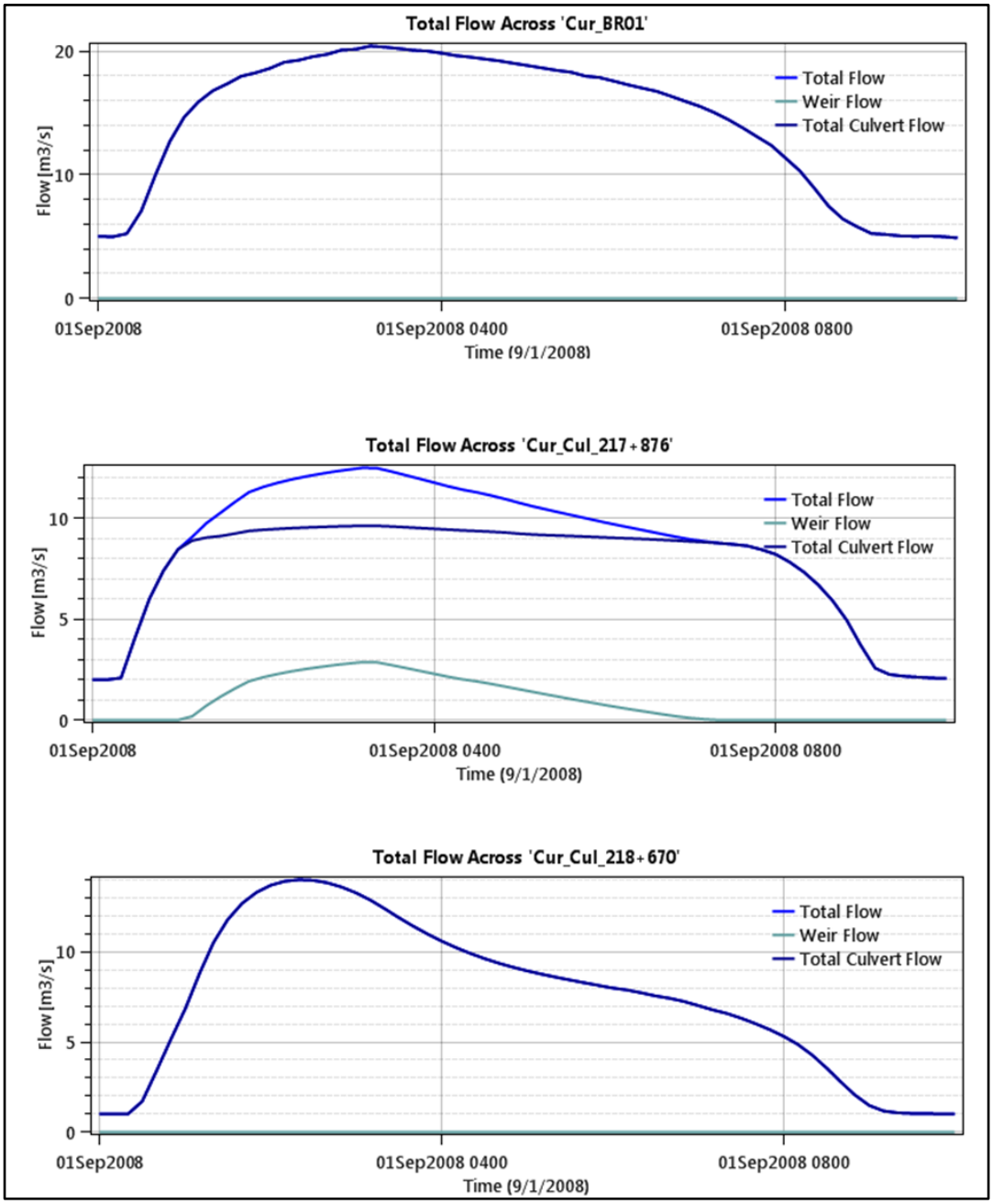

Figure 4.20. Discharge capacity or existing hydraulic structures

4.4.2. Analysis of the Proposed Design

4.4.2.1. Analysis of the Proposed Design with Existing Conditions

In this section, the effect of the railroad embankment between the 216+000 and 219+000 kilometers of the railway line planned is evaluated for a 100-year return

period flood. In addition, the sufficiency of culverts with one barrel at 217+876 (diameter of 2.94 m) and culvert with two barrels at 218+670 (a diameter of 2.94 m), and a “conspan-arc” culvert at 217+868 is controlled. The main purpose of these structures is to ensure proper drainage of the MDM railway, which will serve as a new barrier in front of the rivers.

As previously described, the model was run using the unsteady flow analysis option. There are no changes in the computational grid area, the calculation cell dimensions, and the calculation time step used in the analysis for the present situation. For simulations, the boundary conditions used for the existing situation are maintained. That is, when flow hydrograph is entered in three mains as the upstream boundary condition, 0.004 value of the terrain slope for the downstream boundary condition is used. After the analysis, the flood depth map in Figure 4.21 was obtained, where the flood inundation boundary obtained for the design case can be seen.

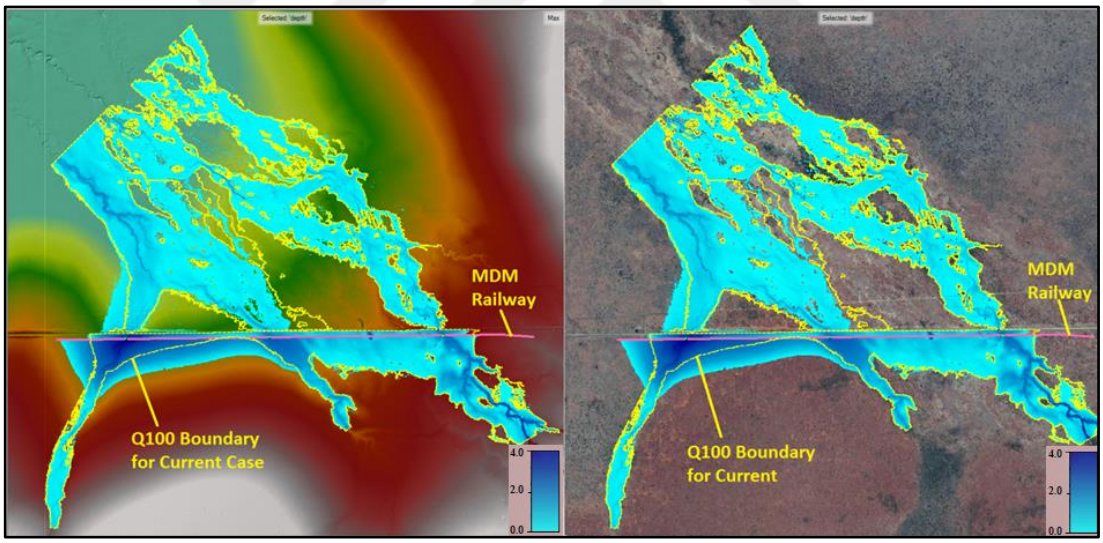

Figure 4.21. Q100 maximum depth map on DTM and aerial photo for design case

After the design case analysis, it is understood that there is no significant change in the flood area in comparison with the existing case. As the water level in upstream has risen because of the designed railway, expansion has also occurred in the inundation area. The flood area of the MDM railway is calculated to be 66.2 ha. An increase of approximately 20.5 ha is observed in this area, which was 45.7 ha for the existing case.

The designed hydraulic structures and profiles passing over the existing structures have been drawn and profiles of the water surface have been drawn to show in detail the change in the water depths of the newly designed railway line.

The location and the water surface of the profile which is taken from the BR01 location are given in Figure 4.24. It is seen that the 15.0 m x 7.0 m "conspan" culvert planned to be constructed on the designed railway creates backwater as low as 0.12 m.

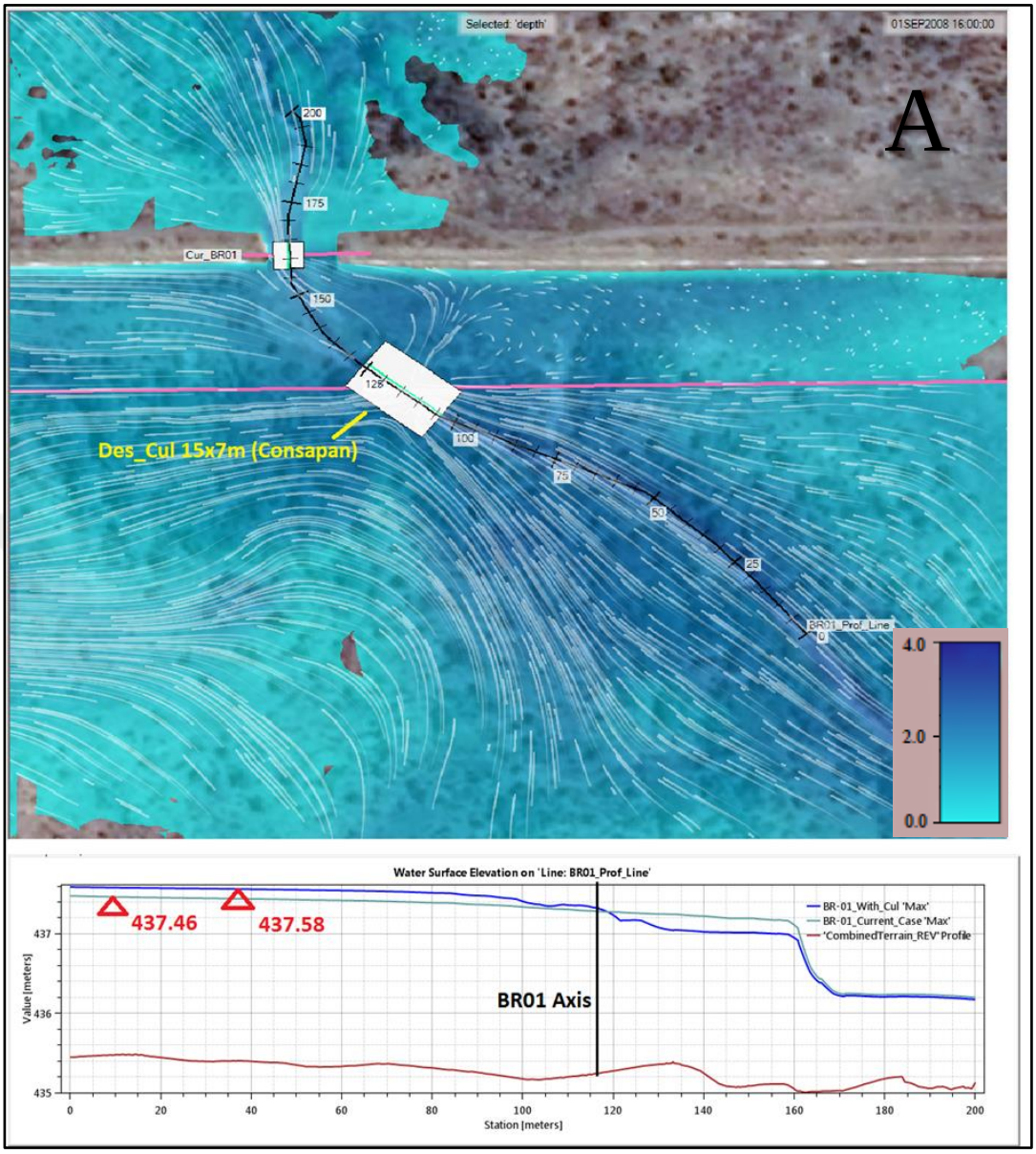

Figure 4.22. Water depth map (m) and velocity vectors; Design and existing case Q_{100} water level profiles for BR01 (A)

The flow rate of the designed BR01 structure is calculated as 39.48 m^3/s at a maximum height as seen in Figure 4.23. The structure with 435.40 m inverts elevation transfers this flow to the downstream with a backwater elevation of 437.46 m. The red line at the BR01 location is 443.34 m and the water flows freely through the BR01 opening.

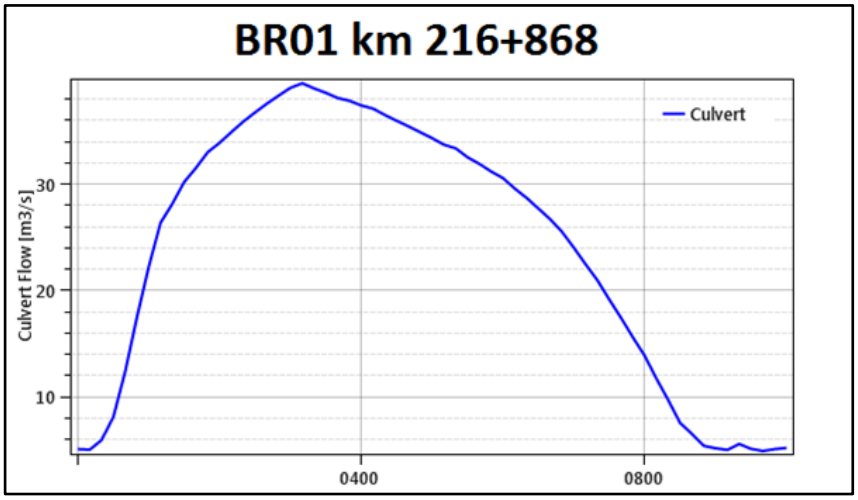

Figure 4.23. Q_{100} flow-time series for BR01

The location and the water surface of the profile which is taken from the culvert location at 217+876 is given in Figure 4.26. It is seen that the water level at the upstream of the 1x2.94 m "circular" culvert planned to be constructed on the railway is 433.26 m. In this region, the designed railway top elevation is 435.59 m. In other words, the water level is 2.33 m below the red line of the railway.

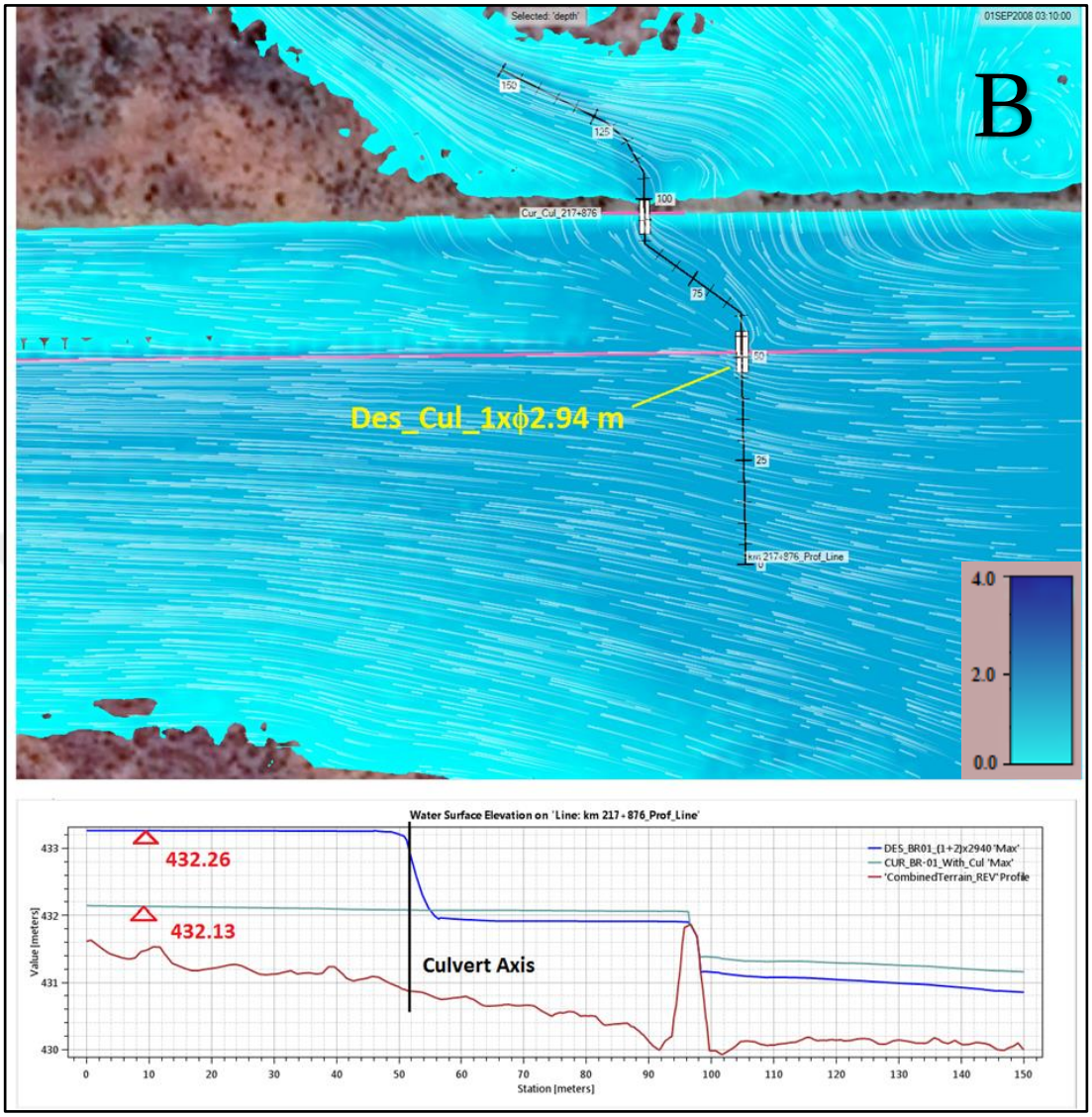

Figure 4.24. Water depth map (m) and velocity vectors; Design and existing case Q_{100} water profiles for km 217+876 (B)

The flow rate of this designed culvert is calculated as 12.29 m^3/s at a maximum height as seen in Figure 4.27. This structure with an inlet invert elevation of 430.90 m passes this flow with the water level of 433.26 m at upstream.

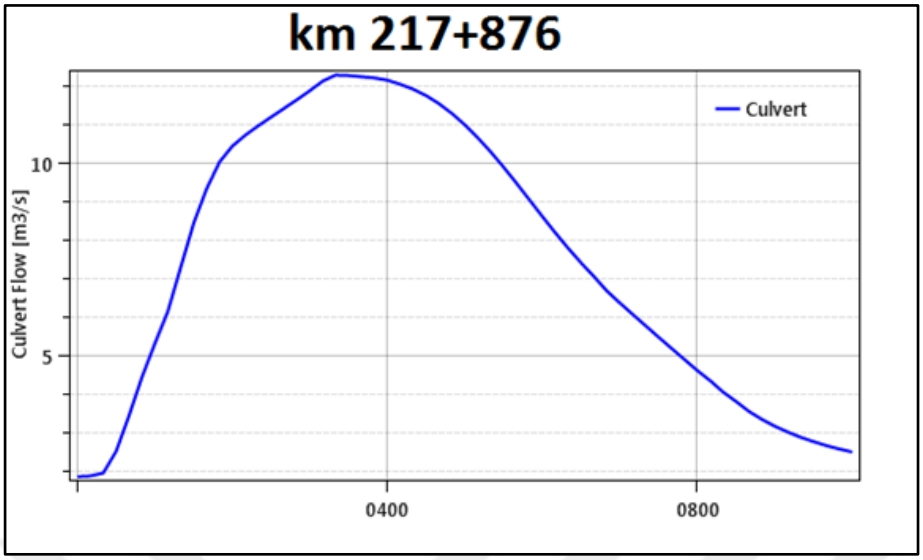

Figure 4.25. Q_{100} flow-time series for km 217+876

The location and the water surface of the profile which is taken from the culvert location at 218+670 are given in Figure 4.28. It is seen that the water level at the upstream of the 2x2.94 m "circular" culverts planned to be constructed on the railway is 433.13 m. In this region, the railway top elevation is 434.35 m. In other words, the water level is 1.22 m below the red line of the railway.

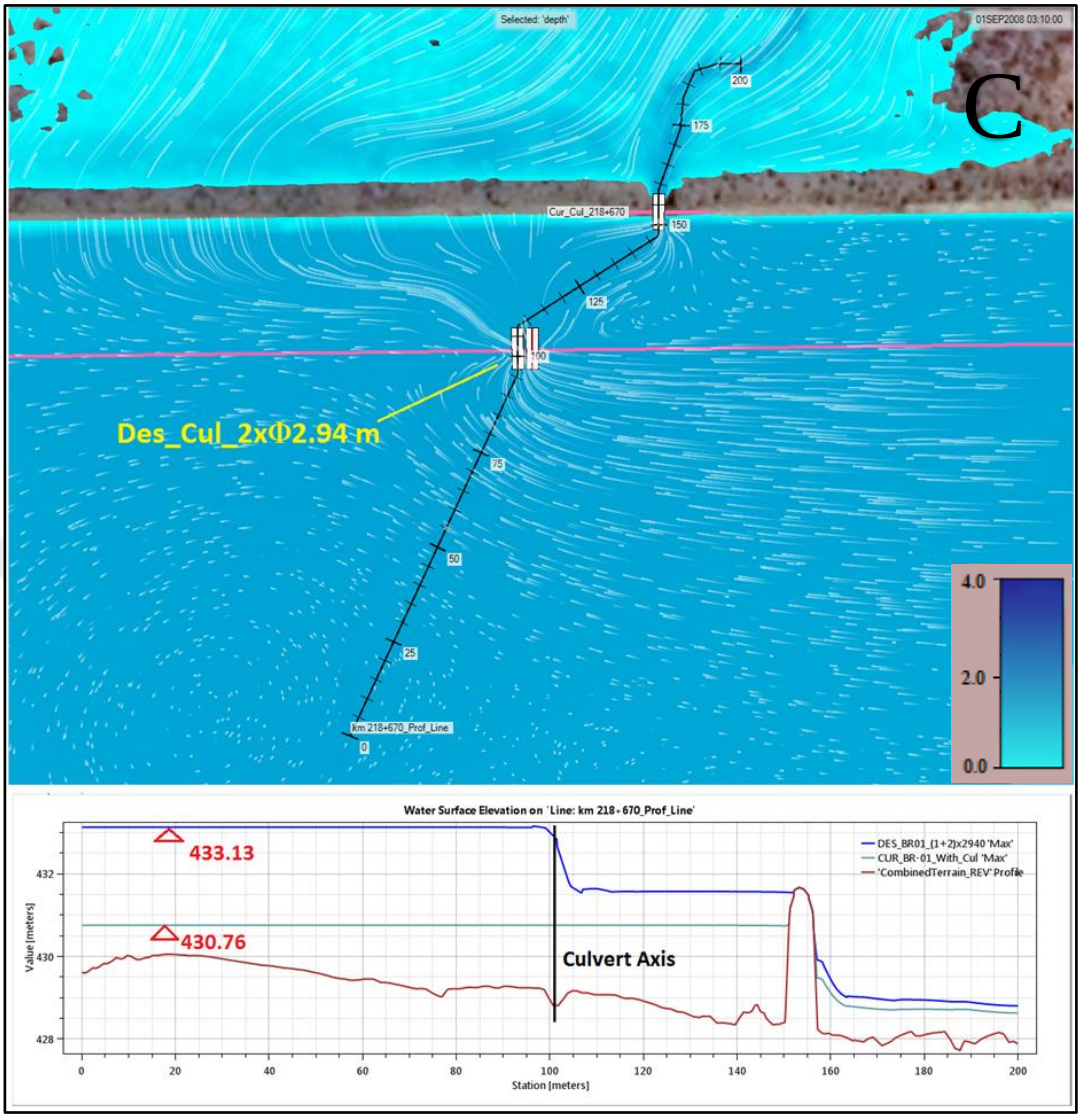

Figure 4.26. Water depth map (m) and velocity vectors; Design and existing case Q_{100} water profiles for km 218+670 (C)

The flow rate of this designed culvert is calculated as 56.17 m^3/s at a maximum height as seen in Figure 4.29. This structure with an inlet invert elevation of 428.90 m passes this flow with the water level of 433.16 m at upstream. Although its own basin has a peak flow value of 13.90 m^3/s, Cur_Cul_218+670 drains 56.17 m^3/s. Because neighbor basins especially feed this lower level basin.

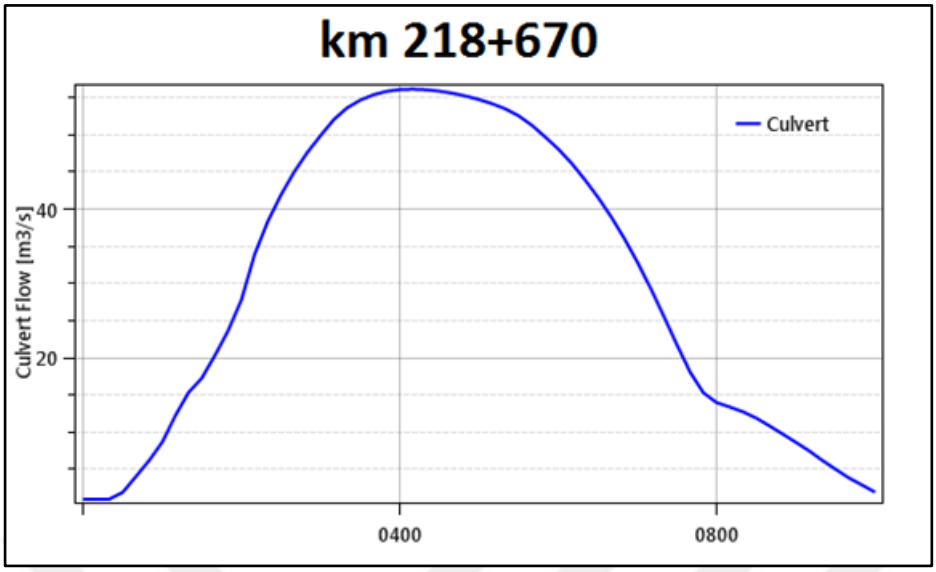

Figure 4.27. Q_{100} flow-time series for km 218+670

A profile of 2745.0 m in length close to the railway embankment was taken to show the relation of the water level with the railroad fill along the railway line. The graph showing the elevation relation between the water surface, natural land and railway fill of this profile line is given in Figure 4.30.

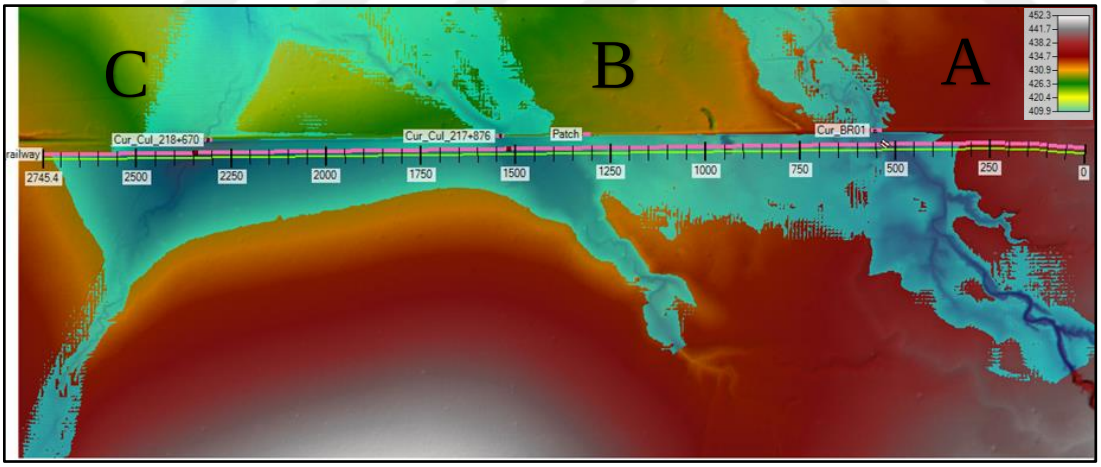

Figure 4.28. Upstream profile along the MDM Railway

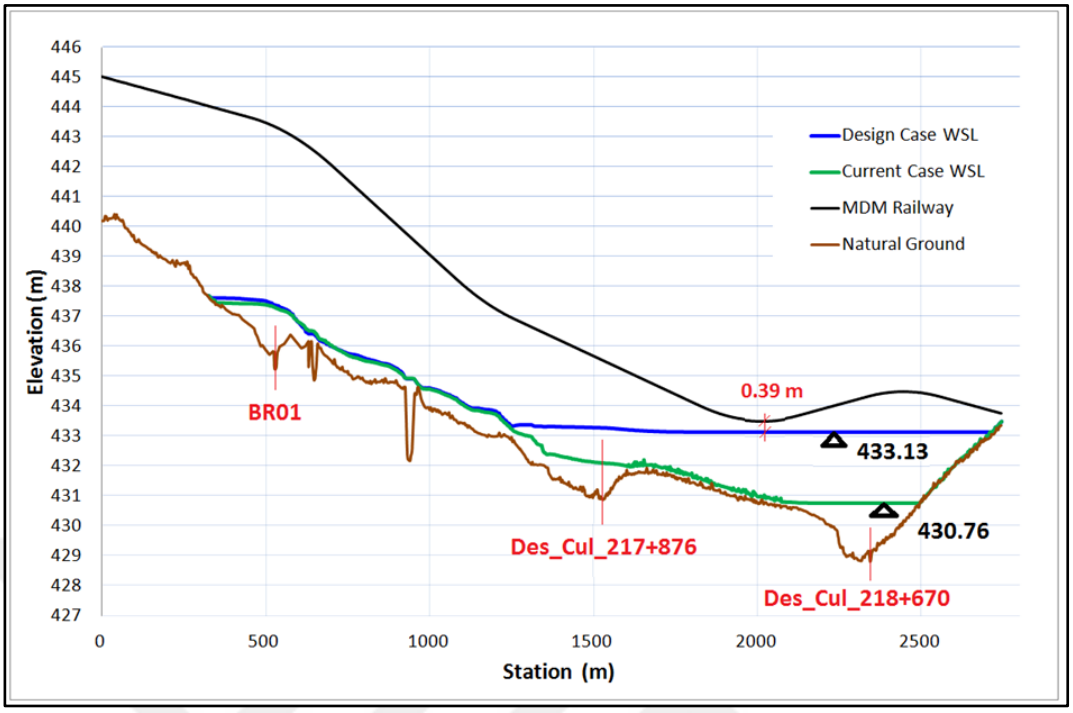

Figure 4.29. Q_{100} max water surface profile along the MDM Railway

In Figure 4.29, when comparing the current case and design case and evaluating the railway elevation in the relevant sections, it is seen that there is no overflow at the existing railway embarkment however only 1/3 of the flood flow at BR01 location passes through the bridges.

4.4.2.2. Analysis of the Proposed Design with Channel Modifications

In this section, different from the design case with current conditions, channelization is introduced to the model (Figure 4.30).

In order to increase the flow passing through the bridges, for the design case, channelization with 15-m bottom width and 2-m rise, a trapezoidal section is applied to the model. Starting from approximately 200 m upstream of the bridges with 0.55% slope and continuing 300 m to the downstream with 0.14% slope, the terrain data is modified.

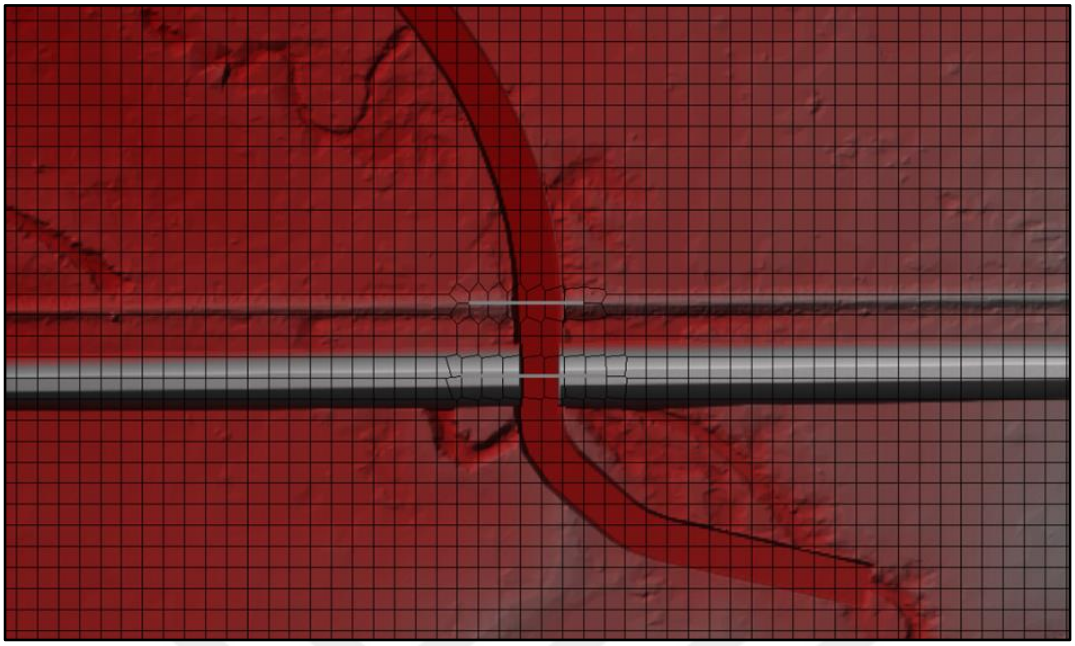

Figure 4.30. Channelization at the bridge location

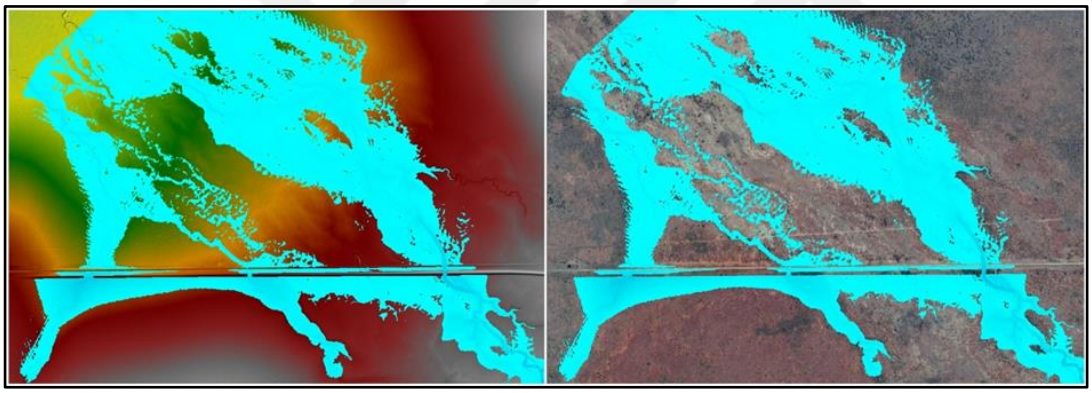

Figure 4.31. Q_{100} max depth map area on DTM and aerial photo for channelized case

The Q_{100} maximum depth map obtained for this model is given in Figure 4.31. As can be understood, there is no significant change in the flood area according to the existing case. As the water level in upstream has lowered because of the newly designed channelization. The flood area of the MDM railway is calculated to be 35.8 ha. A decrease of approximately 9.9 ha is observed in this area, which is 45.7 ha for the existing case.

Newly designed hydraulic structures and profiles passing over the existing structures have been drawn and profiles of the water surface have been drawn to show in detail the change in the water depths of the newly designed railway line.

A dyke is introduced at the upstream of the channelization to increase the flow passing through the bridges. Water surface levels for the cases “with dyke” and “without dyke” is given in Figure 4.34 and for the 2350-m section given in Figure 4.33. It is observed that the water surface elevation is dropped approximately 0.4 m along with the profile.

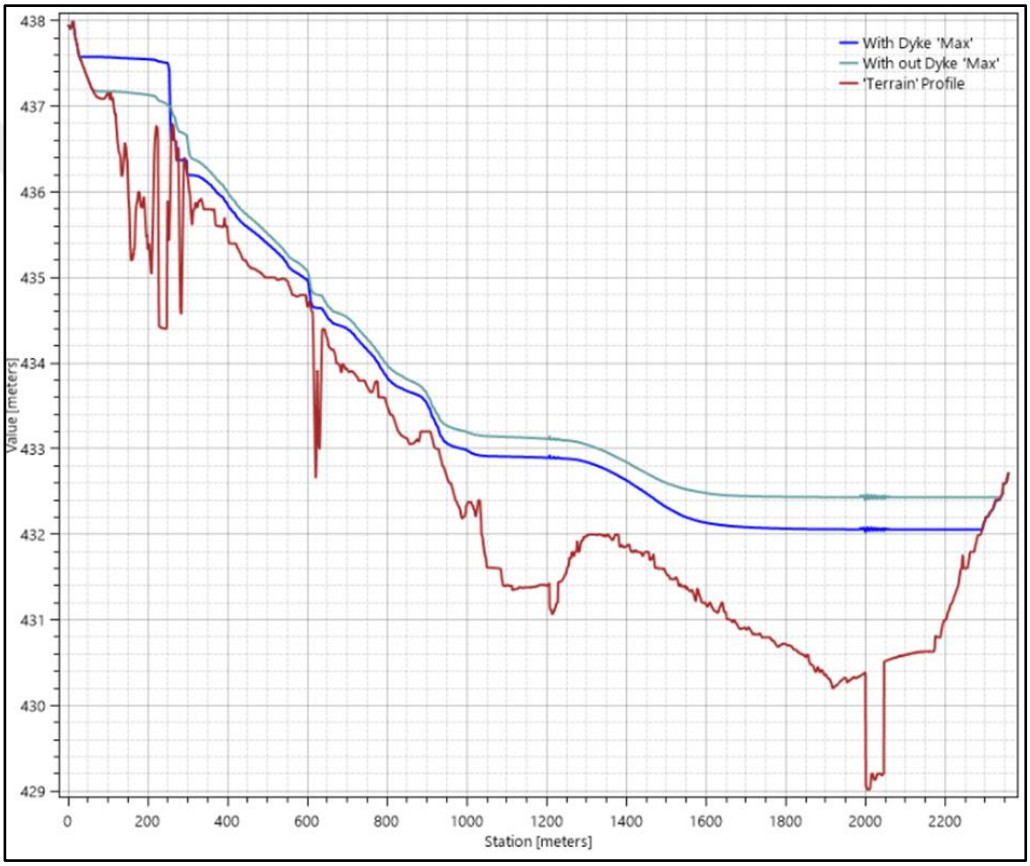

Figure 4.32. Design case Q_{100} max water level comparison for dyke

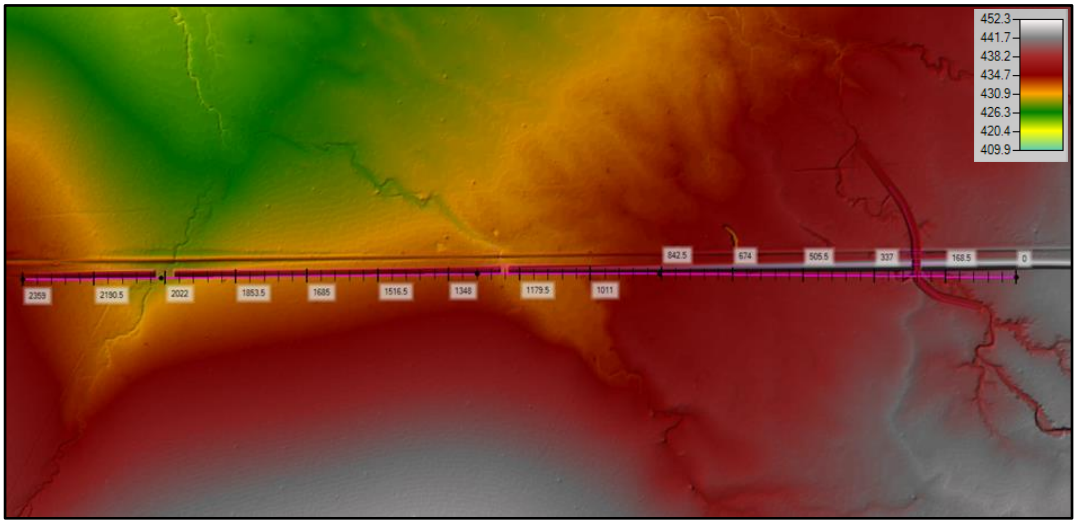

Figure 4.33. Design case Q_{100} max water level profile for BR01

The flow rate of the designed BR01 structure is calculated as 89.82 m^3/s at a maximum height as seen in Figure 4.34. The structure with 434.30 m invert elevation transfers this flow to the downstream with a backwater elevation of 437.55 m. The Top of Rail (TOR) elevation of SGR at the BR01 location is 443.34 m and the water flows freely through the BR01 opening.

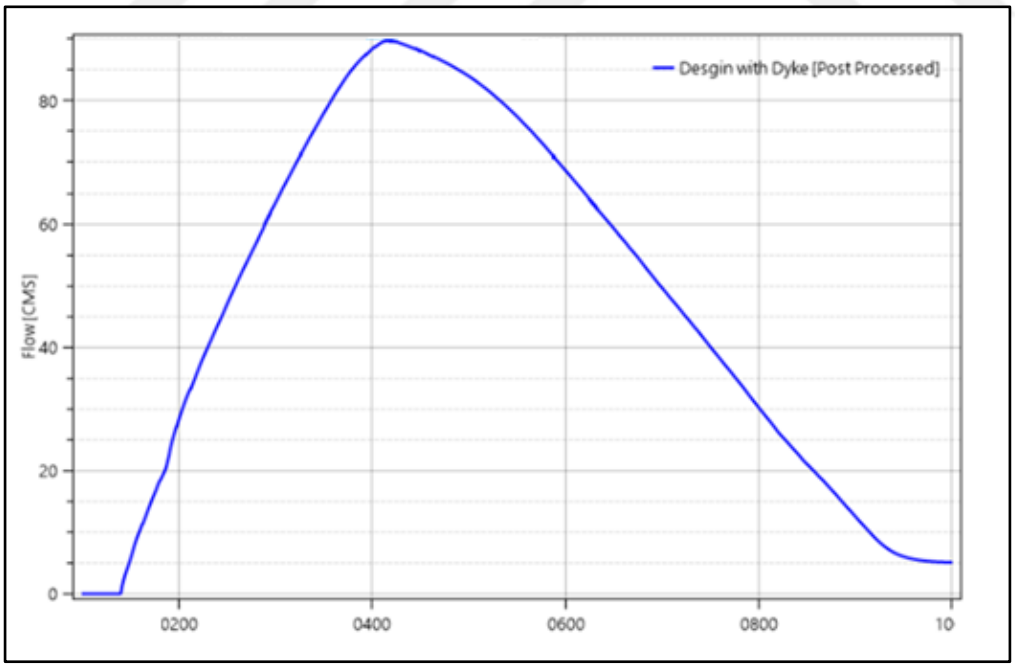

Figure 4.34. Q_{100} flow-time series for BR01

The location and the water surface of the profile which is taken from the culvert location at 217+874 is given in Figure 4.35. It is seen that the water level at the upstream of the 1x2.94 m "circular" culvert planned to be constructed on the railway is 432.84 m. In this region, the designed railway top elevation is 435.59 m. In other words, the water level is 2.75 m below the SGR top of rail elevation, and it is adequate.

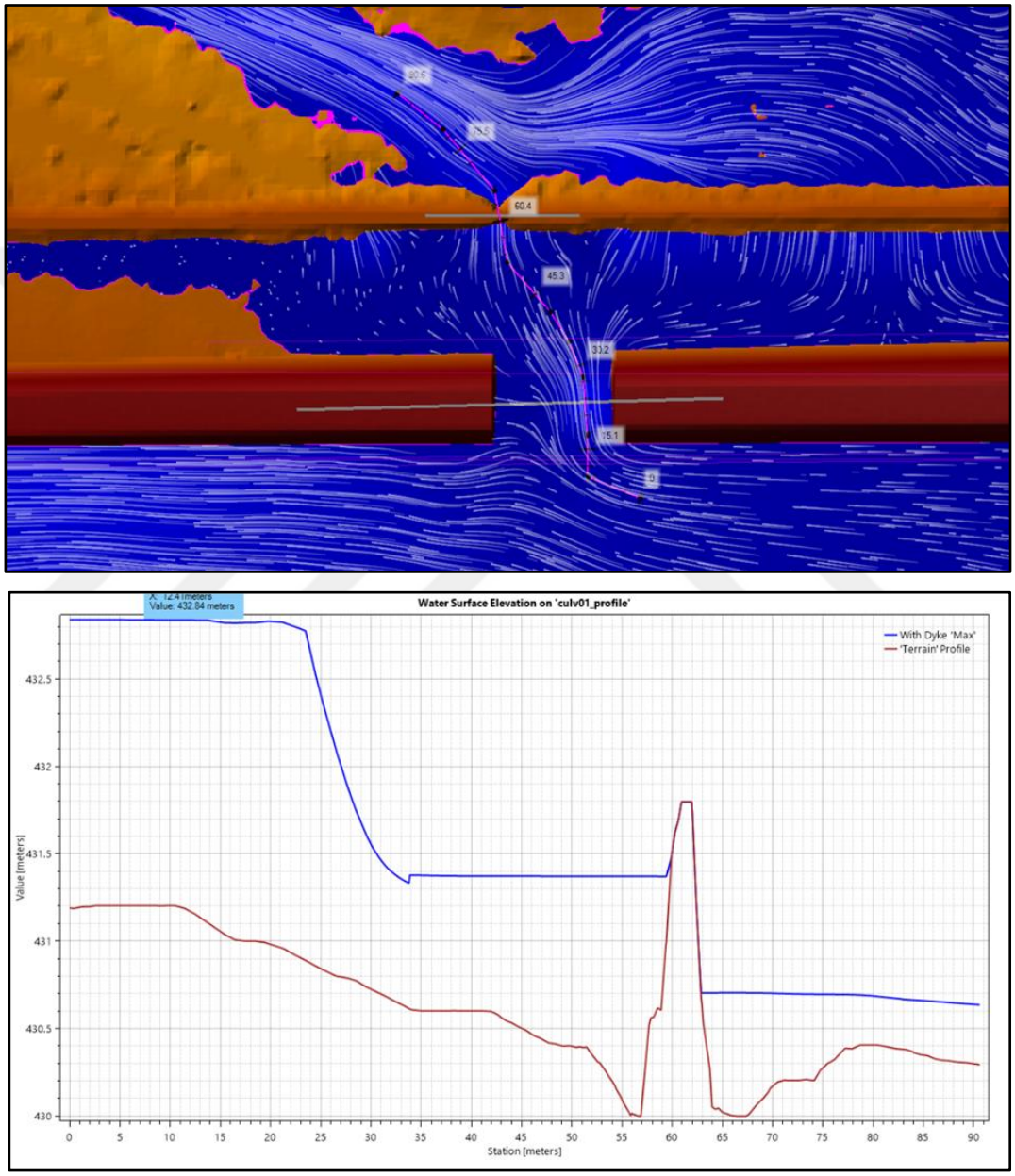

Figure 4.35. Q_{100} max water level profiles for KM 217+874

The flow rate of this designed culvert is calculated as 6.21 m^3/s at amaximum height as seen in Figure 4.38. This structure with an inlet invert elevation of 430.90 m passes this flow with the water level of 432.84 m at upstream.

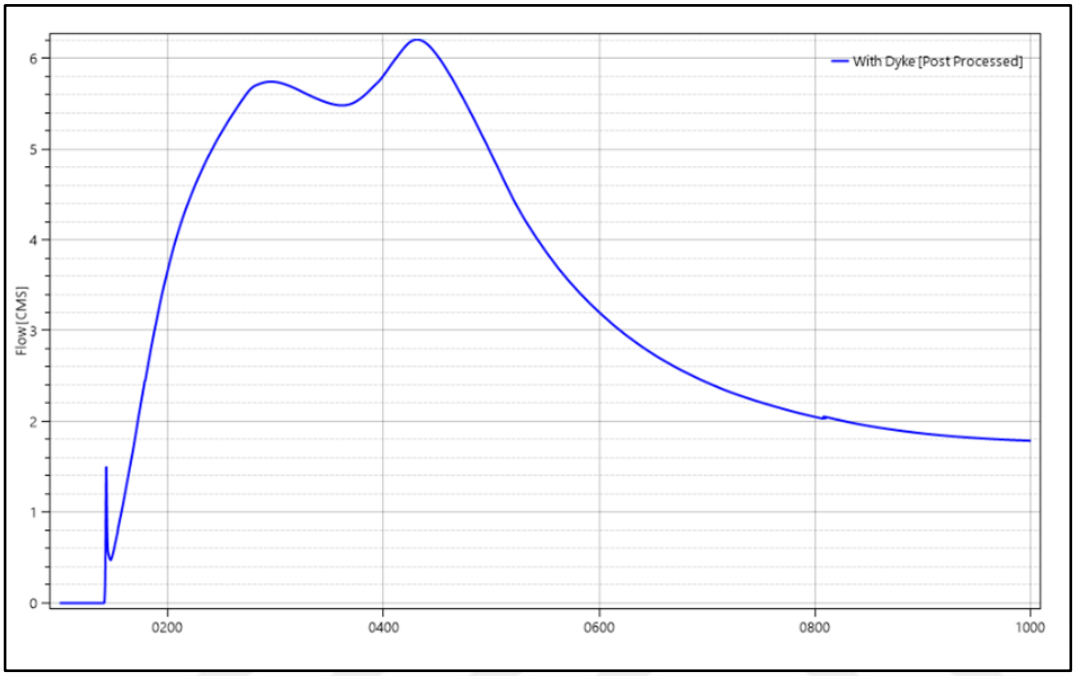

Figure 4.36. Design Q_{100} flow-time series for km 217+874

The location and the water surface of the profile which is taken from the culvert location at 218+670 is given in Figure 4.39. It is seen that the water level at the upstream of the 2x2.94 m "circular" culverts planned to be constructed on the railway is 432.06 m. In this region, the railway top elevation is 434.35 m. In other words, the water level is 2.29 m below the SGR TOR elevation.

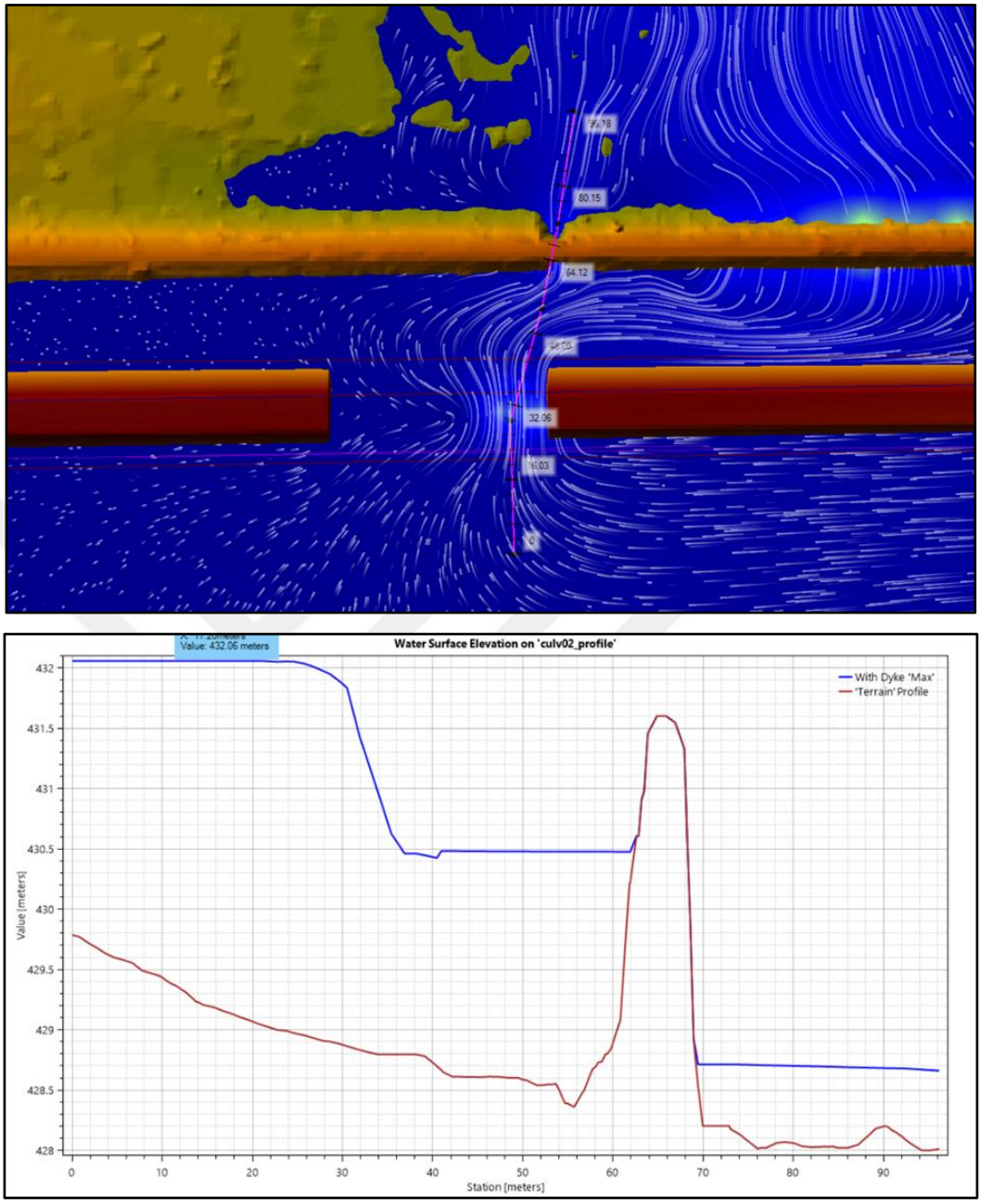

Figure 4.37. Design case Q_{100} max water level profiles for km 218+670

The flow rate of this designed culvert at km 218+670 is calculated as 26.70 m^3/s at maximum height. This structure with an inlet invert elevation of 428.90 m passes this flow with the water level of 433.16 m at upstream. Although its own basin has a peak flow value of 13.90 m^3/s, Cur_Cul_218+670 drains 26.70 m^3/s. Because diverted flow from BR01, the peak flow at this culvert increased by 12.8 m^3/s.

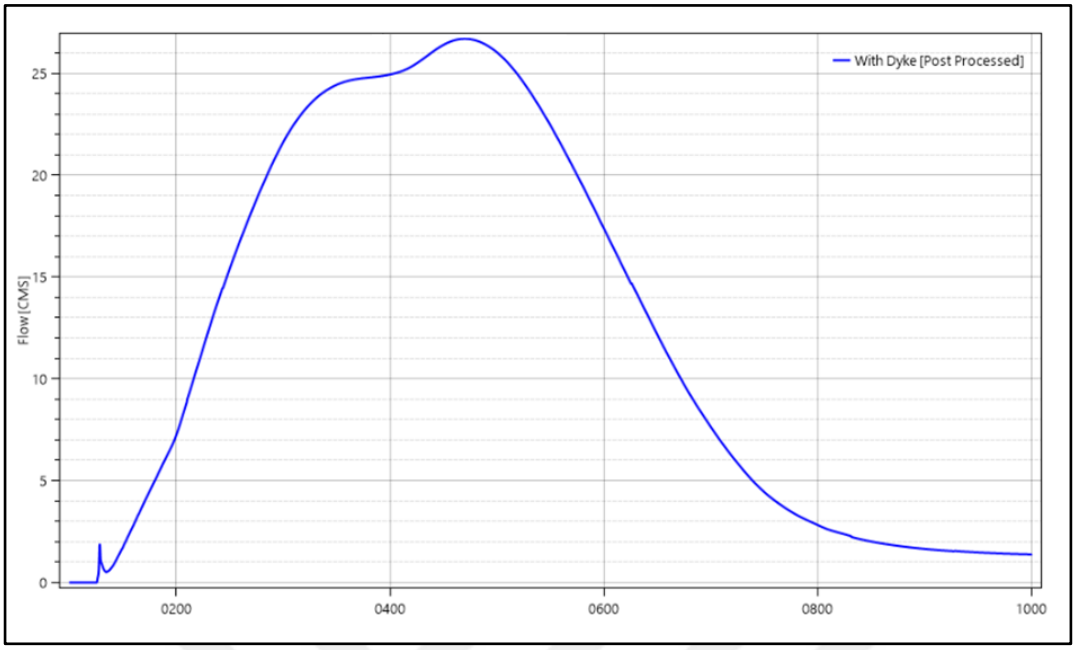

Figure 4.38. Q_{100} flow-time series for km 218+670

A profile of 2745.0 m in length close to the railway embankment was taken to show the relation of the water level with the railroad embankment along the railway line. The graph showing the elevation relation between the water surface, existing ground and railway fill of this profile line is given in Figure 4.39 and Figure 4.40.

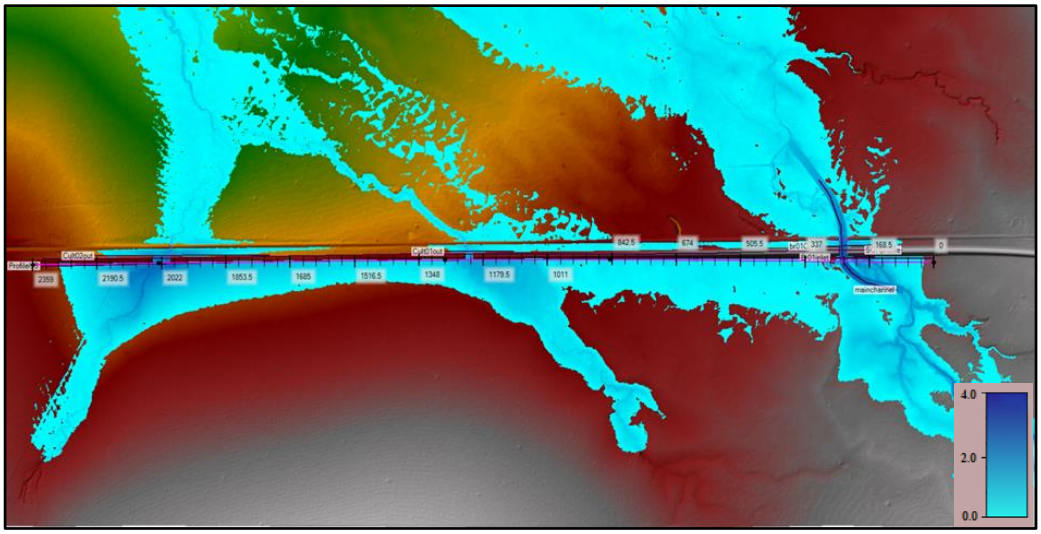

Figure 4.39. Upstream profile along the MDM railway

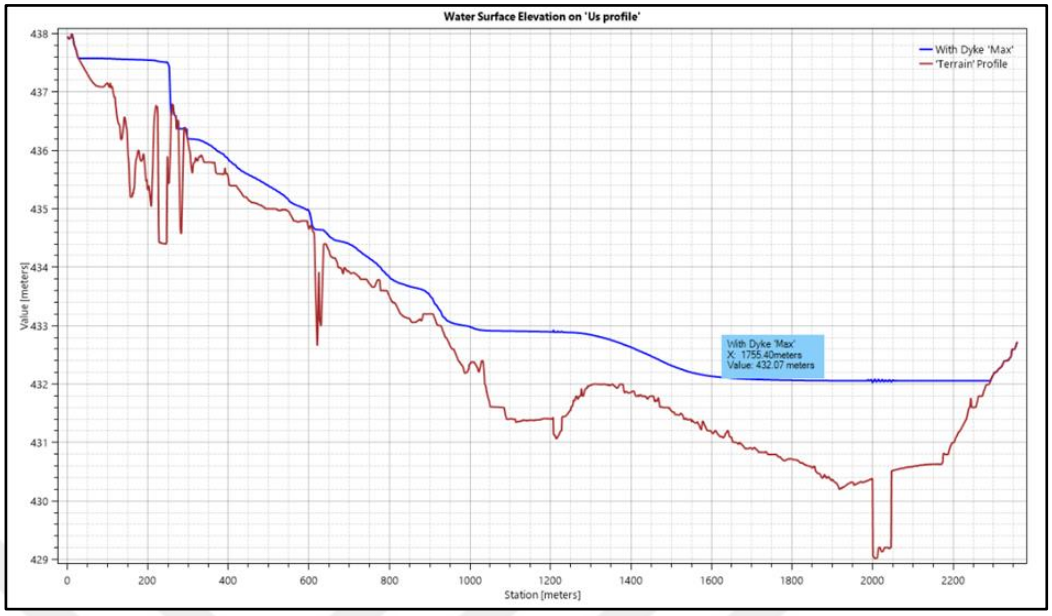

Figure 4.40. Q_{100} max water surface profile along the MDM railway

At the lowest point of the designed SGR profile (433.52), the water surface elevation is 432.07 which is 1.45 m lower than the TOR of SGR. In these profiles, when comparing the current case and design case and evaluating the railway elevation in the relevant sections, it is seen that there is no overflow at the existing railway embankment, and the dimensions of the designed hydraulic structures are appropriate.

4.5. Discussion of the Results

BR01 bridge with a 15-m span, which is the same as the existing bridge at 216+888, is placed on the railway line to be constructed between Morogoro and Makutupora. In the analysis of the simulations, it is understood that the existing bridge is significantly filled and its capacity is decreased. Due to this decrease in capacity, more than 2/3 of the peak flood diverted to the bridge are a crossover from the left bank of the river to the other basins. The construction of the BR01 bridge, which is planned to be built on a new railway designed parallel to the existing railway, does not change this situation. To prevent this problem, channelization with 15-m width and 2-m depth is applied to the model. In this modified case, most of the flood flow passed through the designed and the current bridges. The culverts at 217+876 and 218+670 are designed to pass

the remaining overflow discharge coming from the BR01 location. Since the times of peak hydrograph values for these culverts differ from flood peak time, there was no need to increase the cross section of the culverts. Nonetheless, a dyke is added to the model at the upstream of the BR01 to decrease the diverted flow towards to the culverts from bridge location which lowered the water level further. The freeboard, the height difference between the top of the bridge opening and the maximum water level of 100-year return period flood is found to be 1.45 cm which is adequate and compatible with the design criteria.

For the regions like Wami River, where there is not any defined channel or riverbed, identifying the appropriate geometry for the model is the biggest challenge. Defining existing and designed structures in proper dimensions and identifying friction loss coefficients are vital tasks to simulate floods properly. In this study, being able to compare the water surface elevations of the simulations with flood marks on the field was very fortunate. Flood marks like dry branches stuck to the trees or washed up soil marks can easily show the flood levels. These clues cannot show the exact flood water depth values. However, they can guide the designer towards more realistic results if the model is strayed away from the actual conditions.

On the other hand, site investigations can help identify the areas with uncertainties when the aerial photos are not clear enough to make any judgment. They may also help find out missing hydraulic structures that cannot be seen on the aerial photos. Even the surveying teams may miss these structures. This is the reason why on-site observations are very crucial since any hydraulic structure may impact the flood model results.

CHAPTER 5

DÜDEN RIVER

Without necessary countermeasures, historical bridges can be damaged by scouring caused by high velocities or overtopping with higher water levels. Common practices to protect historical bridges abiding by their origins are riverbed modification and stream redirection. In this study, both practices were considered for protection of the Düden bridge which is known that it has safely functioned and served for so many centuries. Figure 5.1 and Figure 5.2 show the current state of the bridge.

Figure 5.1. The current state of the Düden (Cırnık) Bridge (upstream side)

Figure 5.2. The current state of the Düden (Cırnık) Bridge (downstream side)

There is a flood protection project for Düden River, approved in 2014 by the Turkish State Hydraulic Works (DSİ) which covers the river section from the Mediterranean Sea 0+000.00 m to a weir at 10+180.00 m. Düden bridge is located at 5+730.00 m. Figure 5.3 shows aerial photos of the site.

Figure 5.3. Aerial photos of Düden River

The designed riverbed section for this project is a 45-m wide trapezoidal channel. Historical Bridge Branch of General Directorate of Highways (KGM) requested additional studies considering the riverbed expansion is insufficient to protect Cırnık Bridge from flood damages. For this motive, three different alternatives suggested.

As the first alternative, the bottom width of the riverbed at the bridge location was enlarged to 65-m. When the 2D model analyses were employed for this scenario, the enlargement was found to be insufficient since overtopping at the upstream of the bridge was observed.

The second alternative was a by-pass channel wide enough to transport all the flood discharge. However, because of the spatial restrictions of the bridge location, the height for possible cross-sections is limited to 4 m. This is due to the presence of another bridge parallel to the Düden Bridge with a surface 4.5 m above the ground level of the riverbed.

On the other hand, freeboard is required over the flood flow by taking account of height limitation and freeboard margin, a channel with a minimum of 26-m width is necessary for a flood discharge of 252 m^3/s. This alternative is not applicable because no land space for a channel with a 26-m span is available. Consequently, it is rejected by KGM (General Directorate of Highways). Nevertheless, by this step, possible maximum channel width that can fit is realized to be 14 m on the left side of the river, looking from downstream to upstream.

5.1. Geographical Data

A rectangular bypass channel with a 14-m bottom width parallel to the Düden River was proposed to share flood flow as the third alternative. The designed trapezoidal riverbed has a stone pitching lining and the bypass channel has a concrete rectangular section for which Manning roughness values considering the materials are given in Table 5.1.

Table 5.1. *Main channel and proposed bypass channel characteristics*

	Type	Bottom Width (m)	Height (m)	Channel Slope	Side Slope
Düden River	Trapezoidal	45.00	4.00	0.0055	1:1
Bypass	Rectangular	14.00	4.00	0.0059	-

Table 5.2. *Land Covers values used in the modelling*

Section	Manning Value
Concrete Bypass	0.016
Stone Pitching Düden River	0.035

HEC-RAS 2D uses both finite difference and finite volume scheme to numerically integrate shallow water equations. The computation time interval, which is used in this scheme, had been selected in such a way that the Courant number is less than 1.0 for an accurate and stable solution. Selecting an adequate time step is a function of the cell size and the velocity of the flow moving through those cells.

Several time steps and mesh sizes were tested to obtain optimal computation time interval which can ensure numerical accuracy and minimize computational time. In the model, 5x5 cells and 1-second computation intervals were used.

The bridge section that created in the geometric data module of the HEC-RAS by considering the existing arch openings as culverts with adequate sizes are given in Figure 5.4. Used geometrical data for the bridge openings and hydraulic loss coefficients and Manning roughness values that taken from the HEC-RAS manual in accordance with the examination of the historical bridge are provided in Table 5.3.

Table 5.3. *Historical Bridge Openings*

Type	Span (m)	Height (m)	Entrance Loss Coeff.	Manning Value
Conspan Arch	3.80	1.90	0.30	0.020
Conspan Arch	2.50	2.30	0.30	0.020
Conspan Arch	5.60	4.40	0.30	0.020
Conspan Arch	6.00	4.50	0.30	0.020
Conspan Arch	5.60	4.30	0.30	0.020

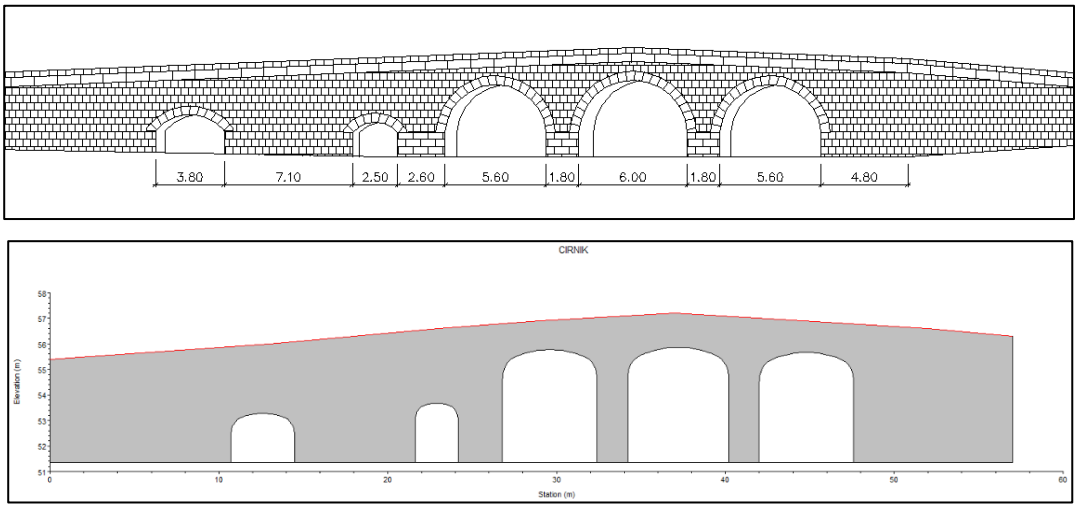

Figure 5.4. Technical drawing and HEC-RAS geometric model of Cırnık Bridge

5.2. Hydrological Data

The flood hydrograph values used in the calculations are taken from the hydrology chapter of the flood protection report of DSİ. The discharge value to be used in flood modeling projects is specified by DSİ as Q_{500}.

Table 5.4. *Düden River Q_{500} discharge values for two sections*

Peak Flood Discharges	**0+000.00 to 0+555.74**	**0+555.74 to 10+790.00**
$Q_{(2)}$	84 m^3/s	83 m^3/s
$Q_{(5)}$	116 m^3/s	114 m^3/s
$Q_{(10)}$	138 m^3/s	136 m^3/s
$Q_{(25)}$	165 m^3/s	163 m^3/s
$Q_{(50)}$	185 m^3/s	183 m^3/s
$Q_{(100)}$	216 m^3/s	205 m^3/s
$Q_{(500)}$	267 m^3/s	252 m^3/s

There are two sets of project flood discharge tables taken from DSİ for the Düden River studies; one is for KM: 0+000.00 to 0+555.74 segment and the other one is for KM: 0+554.74 to 10+790.00 segment. Since the bridge is located at KM: 5+730.00, the flood peak value with a 500-year return period expected in the Düden Bridge is 252 m^3/s. The input hydrograph is given in Figure 5.5.

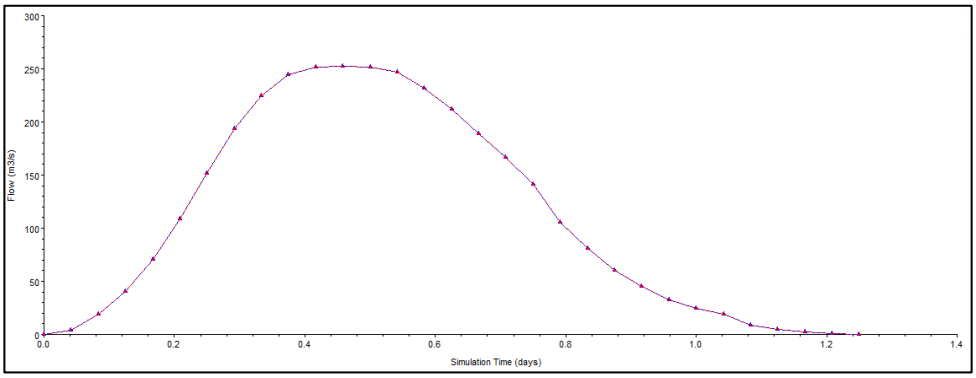

Figure 5.5. Input flood hydrograph of Düden River at the bridge section

5.3. Discussion of the Results

Two-dimensional analyses have been carried out for simulating the extreme flood case using the above-described terrain model and boundary conditions with Q_{500} computation. Figure 5.6 shows the flood discharge passing through the bypass channel.

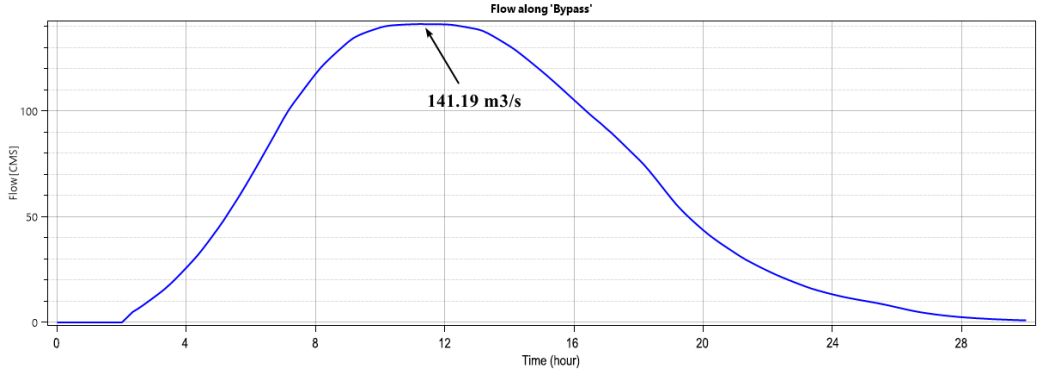

Figure 5.6. The flood discharge at the bypass channel (141.19 m^3/s)

The computed maximum water depths and flood velocities of the model on digital elevation are shown in Figure 5.7 and Figure 5.8. The velocity at upstream and downstream of the study area is 1.70 m/s and constant. Diverted flow from the main channel flows in a higher velocity in the bypass channel. With lower roughness value and steeper channel slope, the velocity along the bypass channel increases up to 3.5 m/s. Meanwhile, the velocity at the historical bridge location drops to 0.70 m/s.

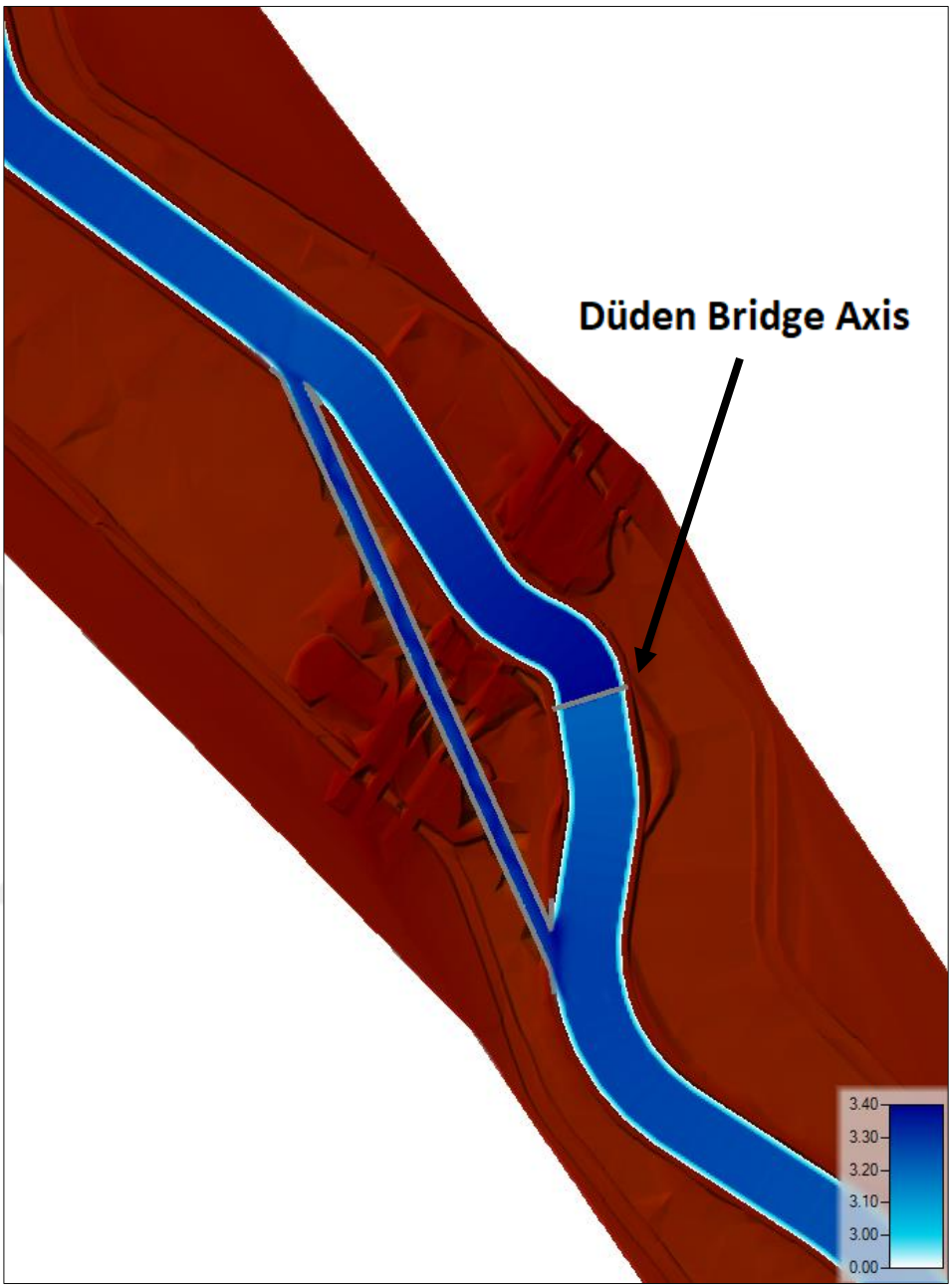

Figure 5.7. Maximum depth map of the flood model (m) (scale 1:50000)

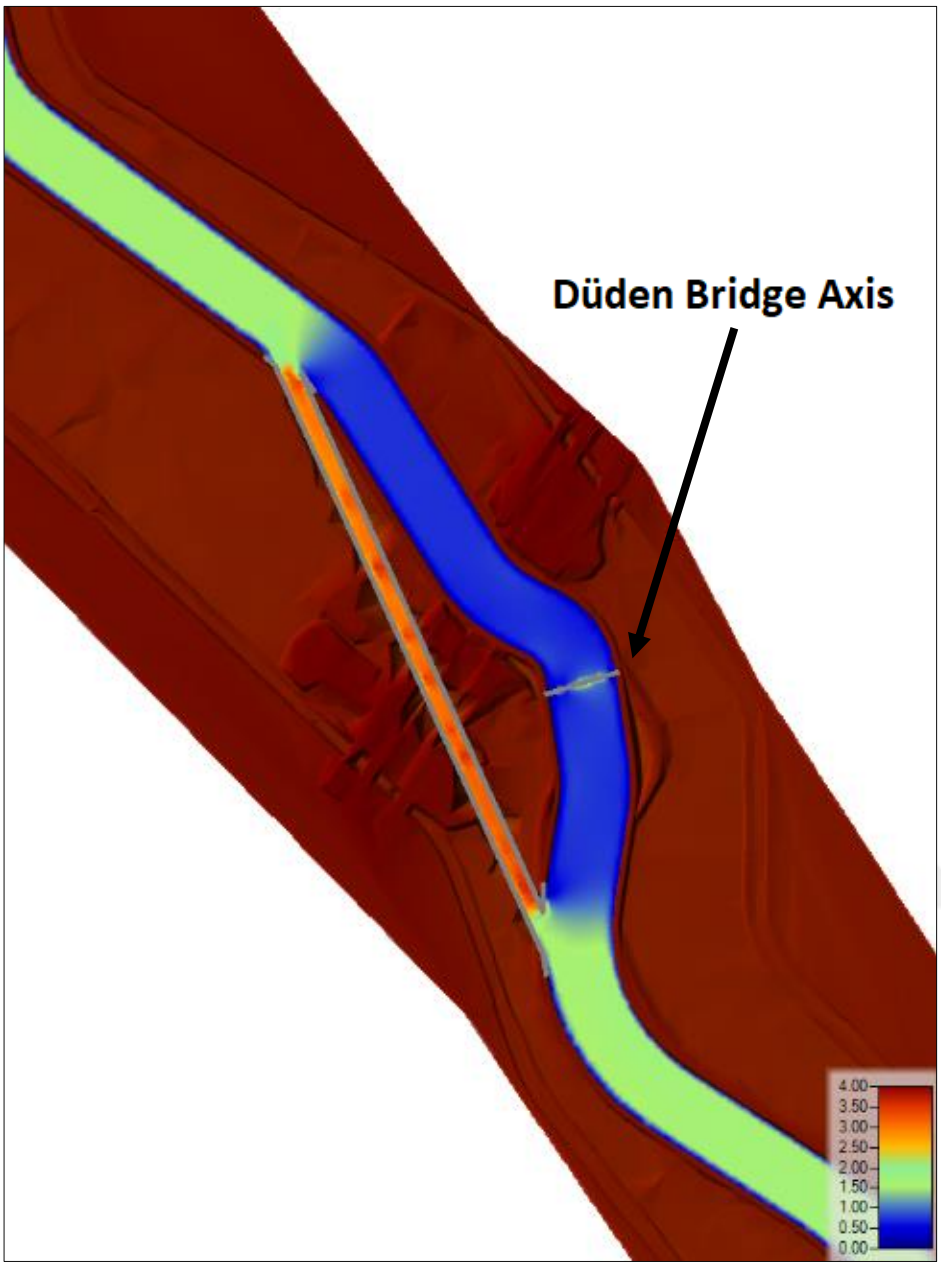

Figure 5.8. Maximum velocity map of the flood model (m/s) (scale 1:50000)

Figure 5.9 shows the flood flow passing through the historical bridge section.

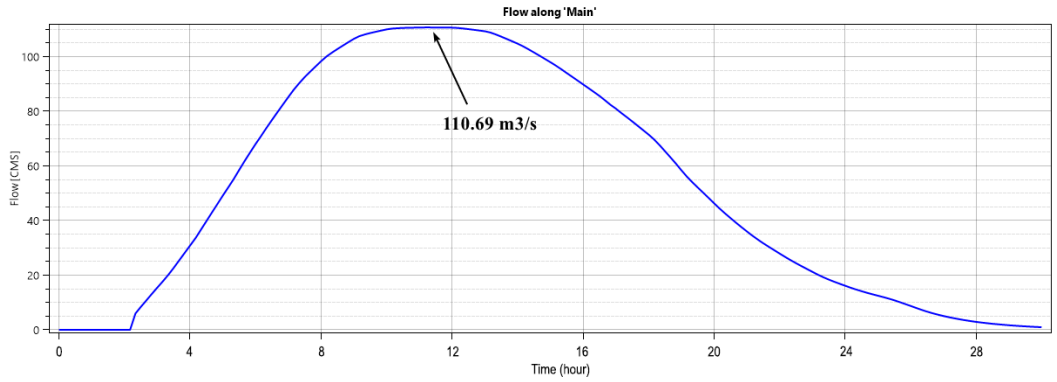

Figure 5.9. The flood discharge at the main channel (110.69 m^3/s)

Figure 5.10 shows the longitudinal water surface profile along the Düden river centerline. It is noted that just upstream of the bridge the water depth is 3.40 m from the riverbed whereas it is 3.21 m just downstream of the bridge.

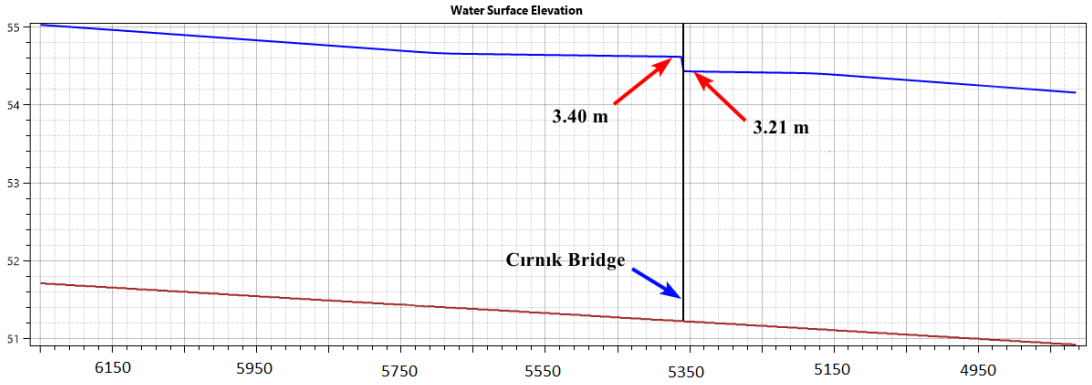

Figure 5.10. Water surface profile along Düden River centerline (m)

As a preliminary study for Düden River, 1D model has been constructed. The water profile of Düden River was subcritical bypass channel with steeper slope and relatively smoother wet surfaces has supercritical profile. HEC-RAS 1D was not adequate to solve parallel channels with different water profiles. The reason was every cross-section of the 1D model had both of the channels geometry and the computations were carried out for only one type of water profile. This is the reason why the flood protection scenarios are also modeled and studied with HEC-RAS 2D in this thesis.

CHAPTER 6

CONCLUSIONS

In this study, the Düden River and Wami River flood problems and protection alternatives were presented with model studies for different alternatives. All the models were created in 2D with HEC-RAS software. Aim of the studies was to understand the existing conditions, determine the inundation boundaries and point out the hydraulically appropriate solutions for the problems.

In the analyses, instead of 1D modeling, 2D modeling is preferred because of the flat topographic characteristics of the regions, absence of defined riverbed for Wami River and parallel channels with different slope profiles for Düden River.

For the Wami Bridge, three scenarios are examined. The starting point of the simulations was the existing case where only the operated bridge is modeled. After that, the design case where the proposed bridge is added to examine the inundation a new railway project may cause. Finally, the modified design case, where channel modification is introduced, which passes through both bridges to transfer most of the flood discharge. The channelization with 15-m width and 2-m depth, the water height at the designed bridge is reduced to 1.45 m and the discharge capacity is increased to 89.92 m^3/sec. In the final simulations, the cell dimensions were 3x3m, relatively smaller compared to the first geometric model of the preliminary simulations, where the cell dimensions were 10x10. The calibration terminated when the usage of smaller cells do not change the flood simulation results significantly.

For Düden Bridge, the first simulation was for the existing case where the historical bridge with insufficient capacity modeled to understand the existing situation. After that, the modified case simulated where an adjoint bypass channel sharing the flood discharge was introduced.

Historical Düden (Cırnık) Bridge with various arch openings is examined for flood protection. According to State Hydraulic Works (DSİ) and General Directorate of Highways (KGM), the cross section of the bridge is insufficient to drain the flood of Düden River. Due to this insufficient capacity, a bypass channel is introduced to divide the flood flow in order to protect the historical bridge from possible flood damages.

460-m long concrete bypass channel with a rectangular cross section designed parallel to the Düden River carrying 141.19 m^3/s of the 500-year return period flood peak value of 252 m^3/s, reducing the main river peak flood discharge to 110.60 m^3/s.

The water surface elevation just upstream of the historical bridge is calculated 54.62 m, corresponding to the water depth of 3.40 m measured from the riverbed elevation of 51.22 m. According to the flood design criteria of DSİ, the required minimum freeboard for bridges is 1.00 m. Considering three of the bridge openings with 4.4 m, 4.5 m and 4.6 m heights, lowering the water depth at the bridge section to 3.40 m is just sufficient.

Considering the present research, the following conclusions can be derived:

The existing circumstance of the Düden River shows that the urbanization and deforestation have a major effect on the flood situation. Expanding the riverbed of Düden River and dividing approximately half of the flood flow with the bypass channel was barely enough to lower the water surface elevation at the historical bridge section to the appropriate level in the simulation.

The existing circumstance of the Wami River shows that without urbanization or deforestation, it can be said that global warming has a major effect on the flood situation. In the existing case simulations, the existing culvert capacities were inadequate and overtopping at these locations was observed.

The design case model studies of Wami River show that in flat regions, usage of a single high capacity bridge is not favorable because the flood starts to spread before swelling at the bridge opening. With low water surface elevations, the discharge

capacity of the bridge cannot be utilized completely. Instead, the application of multiple smaller hydraulic structures for these flat flood regions is considered more appropriate.

REFERENCES

Bates, P. D., & De Roo, A. P. J. (2000). A simple raster-based model for flood inundation simulation. *Journal of Hydrology*, *236*(1–2), 54–77. https://doi.org/10.1016/S0022-1694(00)00278-X

Betsholtz, A., & Nordlöf, B. (2017). Potentials and limitations of 1D, 2D and coupled 1D-2D flood modelling in HEC-RAS: A case study on Höje river. *Lund University*, 128.

Bostan, P. A., Heuvelink, G. B. M., & Akyurek, S. Z. (2012). Comparison of regression and kriging techniques for mapping the average annual precipitation of Turkey. *International Journal of Applied Earth Observation and Geoinformation*. https://doi.org/10.1016/j.jag.2012.04.010

Casulli, V. (2009). A high-resolution wetting and drying algorithm for free-surface hydrodynamics. *International Journal for Numerical Methods in Fluids*. https://doi.org/10.1002/fld.1896

Chow, V. T. (1959). *Open Channel Hydraulics*. New York: McGraw-Hill.

Colgan, A., & Ludwig, R. (2016). Digital terrain model. In *Regional Assessment of Global Change Impacts: The Project GLOWA-Danube*. https://doi.org/10.1007/978-3-319-16751-0_7

Cunge, J. A., Holly, F. M., & Verwey, A. (1980). *Practical aspects of computational river hydraulics.*

Fiddes, D. (1976). *The TRRL East African Flood Model*.

Kıyıcı, E. (2019). *Sensitivity Analysis of 2-D Flood Inundation Model LISFLOOD-FP with Respect to Spatial Resolution and Roughness Parameter*. Middle East Technical University.

Mino, T., Tanaka, Y., Sakamoto, M., & Fujita, T. (2006). Development of praline derived chiral aminophosphine ligands for palladium -catalyzed asymmetric allylic alkylation. *Yuki Gosei Kagaku Kyokaishi/Journal of Synthetic Organic Chemistry*, *64*(6), 628–638. https://doi.org/10.5059/yukigoseikyokaishi.64.628

Mišík, M., Bajčan, J., Sklenář, P. & Kučera M. (2013). Hydrodynamic simulation of Flooding Scenarios for Crisis Management in Prague. *13th International Symposium on Water Management and Hydraulic Engineering*.

Neal, J., Schumann, G., Bates, P., (2012). A subgrid channel model for simulating river hydraulics and floodplain inundation over large and data sparse areas, *Water Resources Research, Vol.48.*

Neelz, S., Pender, G., & Wright, N. G. (2010). Benchmarking of 2D Hydraulic Modelling Packages protecting and improving the environment in England and. In *Benchmarking*.

Işcen, B. N., Yilmaz, B., Aydin, I., & Öktem, N. (2017). On the use of shallow water equations in hydraulics. *Teknik Dergi/Technical Journal of Turkish Chamber of Civil Engineers*, *28*(1), 7747–7764.

Nimaev, A., (2015). *The use of simple inertial formulation of the shallow water equations in 2-D flood inundation modeling.* The Graduate School of Natural and Applied Sciences of Middle East Technical University.

Onuşluel., G. (2005). *Floodplain Management based on the HEC-RAS Modeling System*., Master Thesis. Dokuz Eylül University, Izmir, Turkey.

Özdemir, H., Neal, J.,Bates, P., & Döker, F. (2013). 1-D and 2-D urban dam-break flood modeling in İstanbul, Turkey. Geophysical Research Abstracts Vol.16, EGU2014-218, EGU General Assembly.

Özdemir, H., Bates, P.D., & de Almeida, G. A. M. (2018). Modeling urban floods at submeter resolution: challenges or opportunities for flood risk management? *Flood risk management,* 855-865

Snead, D. B. (2000). *Development and application of unsteady flow models using geographic information systems*. Master Thesis. University of Texas at Austin, Texas.

USACE. (2016). HEC-RAS River Analysis System - Hydraulic Reference Manual, Version 5.0. *Hydrologic Engineering Centre (HEC), U. S. Army Corps of Engineers*, (February), 547. https://doi.org/CPD-68

Vlek, C. A. J. (1996). A multi-level, multi-stage and multi-attribute perspective on risk assessment, decision-making and risk control. *Risk Decision and Policy*. https://doi.org/10.1080/135753096348772

Yanar, T. A., & Akyürek, Z. (2006). The enhancement of the cell-based GIS analyses

with fuzzy processing capabilities. *Information Sciences*. https://doi.org/10.1016/j.ins.2005.02.006

Yeğin, M. (2015). *Flood Risk Mapping Using Economic, Environmental and Social Dimensions*. Middle East Technical University.